AD-A136 056 FRACTURE BEHAVIOR UNDER IMPACT(U) FRAUNHOFER-INST FUER WERKSTOFFMECHANIK FREIBURG (GERMANY F R) J F KALTHOFF ET AL. JAN 83 W-10/83 DAJA37-81-C-0013 1/1

UNCLASSIFIED F/G 20/11 NL

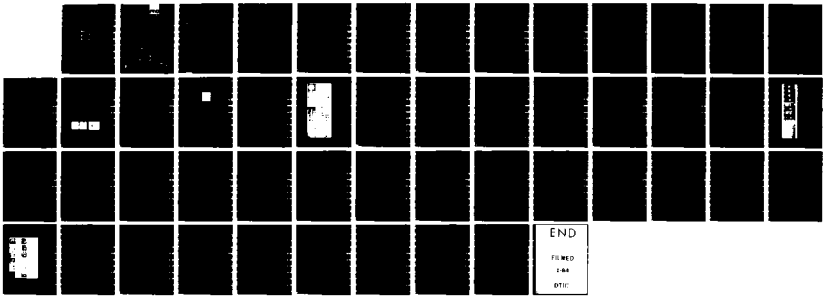

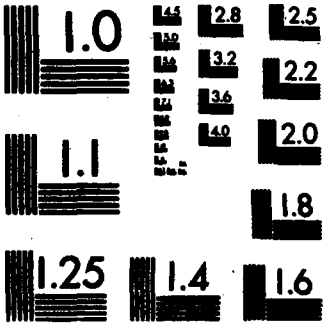

MICROCOPY RESOLUTION TEST CHART
NATIONAL BUREAU OF STANDARDS-1963-A

AD-A136056

(5)

FhG

Fraunhofer-Gesellschaft

FRACTURE BEHAVIOR UNDER IMPACT

W 10/83

Second Annual Report

by

J.F. Kalthoff and S. Winkler

Reporting Period Feb. 1982 - Jan. 1983

Fraunhofer-Institut
für Werkstoffmechanik

SECURITY CLASSIFICATION OF THIS PAGE (When Data Entered)

R&D 3012-MS

REPORT DOCUMENTATION PAGE

READ INSTRUCTIONS BEFORE COMPLETING FORM

1. REPORT NUMBER	2. GOVT ACCESSION NO. AD-A136 058
	3. RECIPIENT'S CATALOG NUMBER
4. TITLE (and Subtitle) Fracture Behavior Under Impact	5. TYPE OF REPORT & PERIOD COVERED Second annual report
	6. PERFORMING ORG. REPORT NUMBER
7. AUTHOR(s) J.F. Kalthoff and S. Winkler	8. CONTRACT OR GRANT NUMBER(s) DAJA37-81-C-0013
9. PERFORMING ORGANIZATION NAME AND ADDRESS Fraunhofer-Institut für Werkstoffmechanik Wöhlerstr 11, 7800 Freiburg/Brsg West Germany	10. PROGRAM ELEMENT, PROJECT, TASK AREA & WORK UNIT NUMBERS 6.11.02A IT161102BH57-06
11. CONTROLLING OFFICE NAME AND ADDRESS USARDSG-UK Box 65 FPO NY 09510	12. REPORT DATE FEB 82 - JAN 83
	13. NUMBER OF PAGES 45
14. MONITORING AGENCY NAME & ADDRESS(if different from Controlling Office)	15. SECURITY CLASS. (of this report) UNCLASSIFIED
	15a. DECLASSIFICATION/DOWNGRADING SCHEDULE

16. DISTRIBUTION STATEMENT (of this Report)

Approved for public release; distribution unlimited.

17. DISTRIBUTION STATEMENT (of the abstract entered in Block 20, if different from Report)

18. SUPPLEMENTARY NOTES

19. KEY WORDS (Continue on reverse side if necessary and identify by block number)

dynamic fracture, impact loading, crack instability, dynamic stress intensity factor, impact fracture toughness, stress optical techniques, shadow optical method of caustics.

20. ABSTRACT (Continue on reverse side if necessary and identify by block number)

The physical behavior of cracks under impact loading is investigated. Single edge cracks or arrays of multiple cracks in rectangular specimens are considered. The specimens are loaded by time dependent tensile stress pulses moving perpendicular to the crack direction. The specimens are directly loaded by an impinging projectile or by a base plate which is accelerated by a projectile. The specimens are made from a transparent model material or a high strength steel. The initial crack lengths and impact velocities are varied throughout the experiments. Utilizing the shadow optical method of caustics in combination

DD FORM 1 JAN 73 1473 EDITION OF 1 NOV 65 IS OBSOLETE

UNCLASSIFIED

SECURITY CLASSIFICATION OF THIS PAGE (When Data Entered)

20) with high speed photography, the dynamic stress intensity factor at onset of rapid crack propagation , i.e. the dynamic fracture toughness K_{Id}, is determined and discussed with regard to the time t_f at which the crack becomes unstable. The results are compared to corresponding static fracture toughness data.

Within the second year of the three years research project many experiments of the proposed main investigations have been carried out:

First the dependence of the impact fracture toughness K_{Id} on loading rate has been investigated. Specimens made from the Araldite B with single edge cracks have been tested under base plate - and under direct impact loading conditions. Within the range of loading rates achieved so far, the measured impact fracture toughness K_{Id} do not show a dependence from loading rate.

The experiments with configurations of multiple cracks exhibit a rather complex time dependent stress intensity factor history. Due to transient effects the early time behavior is very different from the static behavior. In particular a periodic exchange of the crack tip strain energy from one crack to the other takes place. Only for long times after impact the overall situation becomes similar to the one under static loading conditions.

The stress intensity factor histories for cracks of different lengths under impact loading has been measured and compared. The data do not show an influence of crack length for early times after impact. Only at later times the larger crack exhibits a larger stress intensity factor, as one expects from static considerations. Thus the parameter "time" controls the fracture behavior under highly dynamic loading conditions and not the length of the crack as in static considerations.

FRAUNHOFER-INSTITUT FÜR WERKSTOFFMECHANIK
Wöhlerstr. 11, D-7800 Freiburg

FRACTURE BEHAVIOR UNDER IMPACT

W 10/83

Second Annual Report

by

J.F. Kalthoff and S. Winkler

Reporting Period Feb. 1982 - Jan. 1983

United States Army

EUROPEAN RESEARCH OFFICE OF THE U.S. Army

London England

CONTRACT NUMBER DAJA 37-81-C-0013

ABSTRACT

The physical behavior of cracks under impact loading is investigated. Single edge cracks or arrays of multiple cracks in rectangular specimens are considered. The specimens are loaded by time dependent tensile stress pulses moving perpendicular to the crack direction. The specimens are directly loaded by an impinging projectile or by a base plate which is accelerated by a projectile. The specimens are made from a transparent model material or a high strength steel. The initial crack lengths and impact velocities are varied throughout the experiments. Utilizing the shadow optical method of caustics in combination with high speed photography, the dynamic stress intensity factors at the tip of the crack are measured as functions of time during the impact event. The critical value of the dynamic stress intensity factor at onset of rapid crack propagation, i.e. the dynamic fracture toughness K_{Id}, is determined and discussed with regard to the time t_f at which the crack becomes unstable. The results are compared to corresponding static fracture toughness data.

Within the second year of the three years research project many experiments of the proposed main investigations have been carried out:

First the dependence of the impact fracture toughness K_{Id} on loading rate has been investigated. Specimens made from Araldite B with single edge cracks have been tested under base plate - and under direct impact loading conditions. Within the range of loading rates achieved so far, the measured impact fracture toughness data K_{Id} do not show a dependence from loading rate.

The experiments with configurations of multiple cracks exhibit a rather complex time dependent stress intensity factor history. Due to transient effects the early time behavior is very different from the static behavior. In particular a periodic exchange of the crack tip strain energy from one crack to the other takes place. Only for long times after impact the overall situation becomes similar to the one under static loading conditions.

The stress intensity factor histories for cracks of different lengths under impact loading has been measured and compared. The data do not show an influence of crack length for early times after impact. Only at later times the larger crack exhibits a larger stress intensity factor, as one expects from static considerations. Thus the parameter "time" controlles the fracture behavior under highly dynamic loading conditions and not the length of the crack as in static considerations.

KEYWORDS: dynamic fracture, impact loading, crack instability, dynamic stress intensity factor, impact fracture toughness, stress optical techniques, shadow optical method of caustics

CONTENTS

1 INTRODUCTION

The failure behavior of structures which contain cracks or crack-like defects in general is very well understood. The concept of fracture mechanics provides a powerful tool for quantitative safety predictions:

- The stress intensity factor, K, is a measure of the severity or criticality of a crack. The main parameters which determine this mechanical property are the length of the crack and the load which is applied to the crack.

- The fracture toughness, K_{Ic}, i.e. the critical stress intensity factor for onset of rapid crack propagation, is a material property which describes the resistance of the material to crack extension.

For static or quasistatic loading conditions this concept has been successfully applied to many cases of practical importance:

- Formulas have been established to determine (exactly or at least approximately) the static stress intensity factor K_I^{stat} for almost any crack problem.

- Standardized test procedures have been developed to measure the static fracture toughness K_{Ic} for different materials.

- Design criteria have been formulated on the basis of these two properties, i.e. K_I^{stat} and K_{Ic}, which allow the assessment of the safety of a structure under the specific service conditions [1,2].

The fracture behavior of cracks subjected to dynamic loading is considerably less well understood. The reason for this situation is the fact that these problems are far more complicated. The stress intensification at the crack tip becomes a complicated function of time and consequently, the instability event is controlled by a rather complex process which cannot be described by simple means.

Thus, the most commonly used dynamic material strength value still is the Charpy energy, i.e. the energy to break a Charpy V-notch specimen in a pendulum type impact tester. This material property represents only a relative material characterisation which cannot be used for quantitative design purposes. Work is performed to develop a test procedure for measuring the dynamic fracture toughness value under impact loading, i.e. the impact fracture toughness K_{Id}. A currently proposed procedure for measuring this quantity in instrumented impact tests [3], however, is based on a simplyfied static evaluation procedure which determines the stress intensity factor from load values measured at the tup of the striking hammer via static stress intensity factor formulas. Fig. 1 compares these static stress intensity factors K_I^{stat} with the actual dynamics stress intensity factors at the crack tip, denoted K_I^{dyn} [4]. The differences are quite large, in particular at early times of the impact event. The differences have not vanished even after a

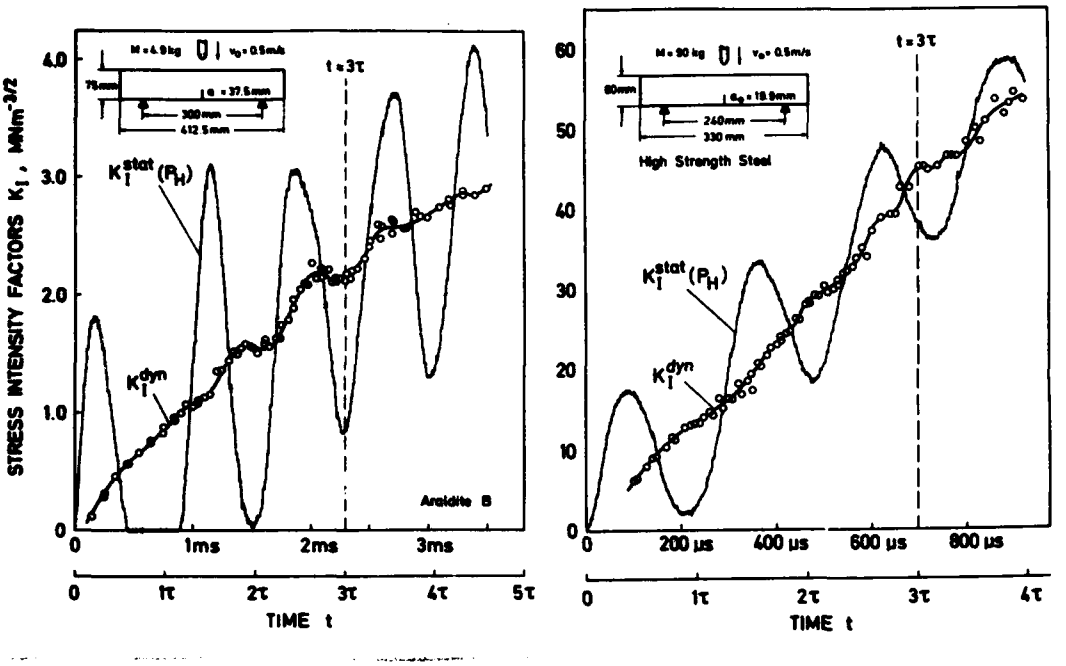

Fig. 1 Stress intensity factors for precracked bend specimens under drop weight loading

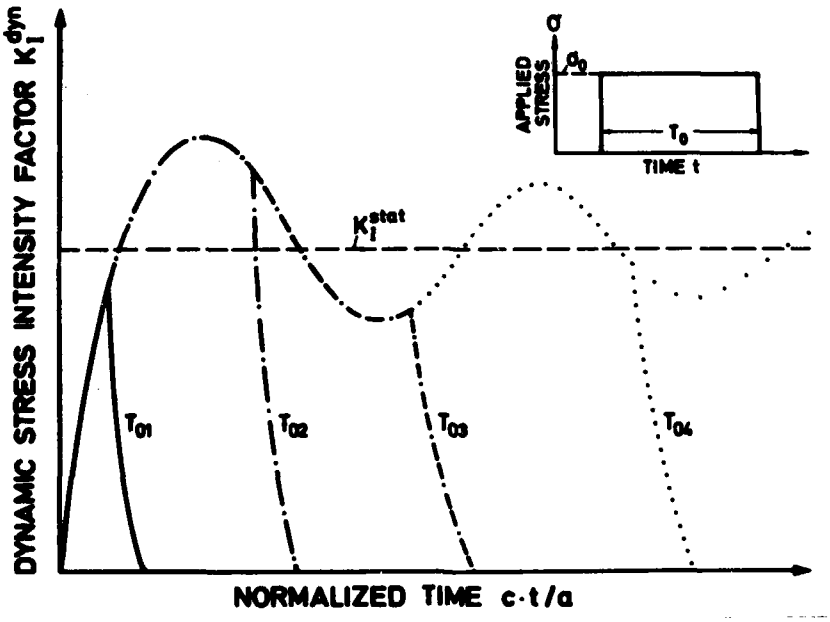

Fig. 2 Dynamic stress intensity factor for a crack under step function loads of durations $T_{o1} < T_{o2} < T_{o3} < T_{o4}$, schematically

time of 3τ, where τ is the period of the eigenoscillation of the specimen (see [3]). This procedure, therefore, is only applicable for very large times to fracture which, however, can only be obtained when the impact velocity is reduced to very low values. Depending on the test conditions the maximum tolerable impact velocity has to be as low as about 1 m/s [3].

Another example which demonstrates the complex behavior of dynamic stress intensifications is shown in Fig. 2. For a crack of length a under mode-I step function load of duration T_0 the dynamic stress intensity factor is plotted as a function of time (see [5-9]). The dimensionless time unit $(c_1 t)/a_0$ is used in this diagram, where c_1 is a wave velocity. K_I^{dyn} increases with time according to a $\sqrt{t}$-dependence, overshoots the equivalent static stress intensity factor K_I^{stat} up to 30%, and for larger times only approaches K_I^{stat} by an oscillation with a damped amplitude. The duration T_0 of the pulse controls the physically valid time interval (see Fig. 2). Because of the complicated $K_I^{dyn}(t)$ behavior, especially for short pulse durations, conclusions on the effective stress intensity factor for the impact event can hardly be made. The maximum value of the $K_I^{dyn}(t)$ curve cannot control the actual instability event, because this value is only active for a very short time and does not allow the crack to make large jumps. On the basis of energy and momentum considerations, Steverding and Lehnigk [10-13] developed a dynamic fracture criterion which correlates the critical crack lengths with the applied pulse durations. A similar but more general criterion was developed later by Kalthoff and Shockey [14-17] denoted as *minimum* time fracture criterion.

These influences of time effects on the stress condition can have severe influences on procedures for measuring dynamic fracture toughness values. Impact fracture toughness data have been measured at different loading rates. Depending on the strain rate sensitivity of the material, K_{Id} decreases more or less strongly with increasing loading rate $\dot{\sigma}_0$, as is indicated in Fig. 3. Most of the dynamic fracture toughness data have been obtained in the lower impact velocity range with Charpy - and drop weight tests. An overview of the results obtained and the problems encountered in measuring these quantities is given in the papers of Turner, Venzi, Shoemaker, Rolfe, Loss, Ireland, Wullert, and others [18-22]. Data at higher loading rates have been measured for example by Costin, Duffy, Freund, and Server [23,24] with Hopkinson bar experiments, by Shockey, Curran, Homma and Kalthoff [17,25-27] with flyer plate impact experiments, and by Ravi Chandar and Knauss [28] using electromagnetic loading techniques. In their papers Eftis and Krafft [29] and Shockey and Curran [25] discuss the interesting question whether a minimum value of K_{Id} exists, which cannot be reduced even if the loading rate would be increased further (see Fig. 3).

The difficulty in all the measuring procedures consists of establishing a relation between quantities measured externally at the test machine and the actual stress intensity factor existing at the tip of the crack in the specimen. Different approaches are used: Simplyfied static ana-

lyses (e.g. with Charpy tests [3]), theoretical analyses which sometimes are based on nonrealistic assumptions (e.g. infinite boundaries or step function loads [5-9]), or numerical analyses which necessarily are very complicated. In this project the problem of deriving the stress intensity factor from secondary quantities measured in an experiment shall be avoided by measuring the actual dynamic stress intensity factor directly at the crack tip by a special optical technique developed at the Fraunhofer-Institut für Werkstoffmechanik, i.e. the shadow optical method of caustics.

The investigations are aimed to generate basic information on the failure behavior of precracked specimens with finite boundaries subjected to dynamic tensile stresses. The results shall be of special importance for the development of improved impact fracture toughness tests and the assessment of the load carrying capacity of structures under dynamic loading conditions in general.

2 GENERAL OUTLINE

2.1 Technical Objectives

The physical behavior of cracks under impact loading is investigated. Single edge cracks or arrays of multiple cracks in rectangular specimens are considered. The specimens are loaded by time dependent tensile stress pulses p(t) moving perpendicular to the crack direction. The pulses are produced by impinging projectiles. The specimens are made from a transparent model material or a high strength steel. Utilizing the shadow optical method of caustics in combination with high speed photography (see Fig. 4), the dynamic stress intensity factors, K_I^{dyn}, at the tip of the crack are measured as functions of time during the impact event. The critical value of the dynamic stress intensity factor at onset of rapid crack propagation, i.e. the dynamic fracture toughness K_{Id}, is determined and compared to the corresponding static fracture toughness K_{Ic}. The results are discussed with regard to the times t_f at which the initial cracks become unstable.
Two kinds of impact experiments are envisaged in the research program:

A) Direct impact loading: The precracked specimen is directly impacted by the projectile. After passage of the compressive stress pulse through the specimen and reflection of the pulse at the free end of the specimen, the crack is loaded by tensile stresses (see schematic drawing - Fig. 5).
B) Base plate loading: The precracked specimen is loaded in tension by a base plate which is accelerated by the impinging projectile (see schematic drawing - Fig. 6).

The investigation of single edge cracks (as shown in the back specimen of Fig. 6) or arrays of multiple cracks (as shown e.g. in the front specimen of Fig. 6) is planned.

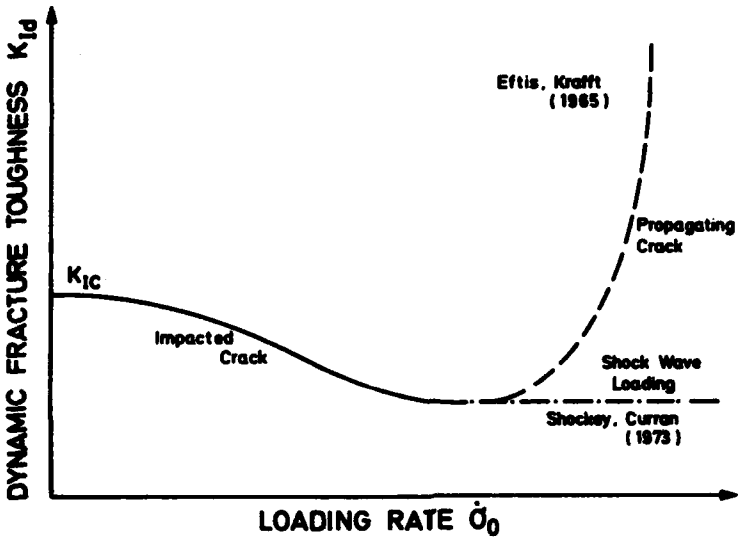

Fig. 3 Dynamic fracture toughness as a function of loading rate, schematically

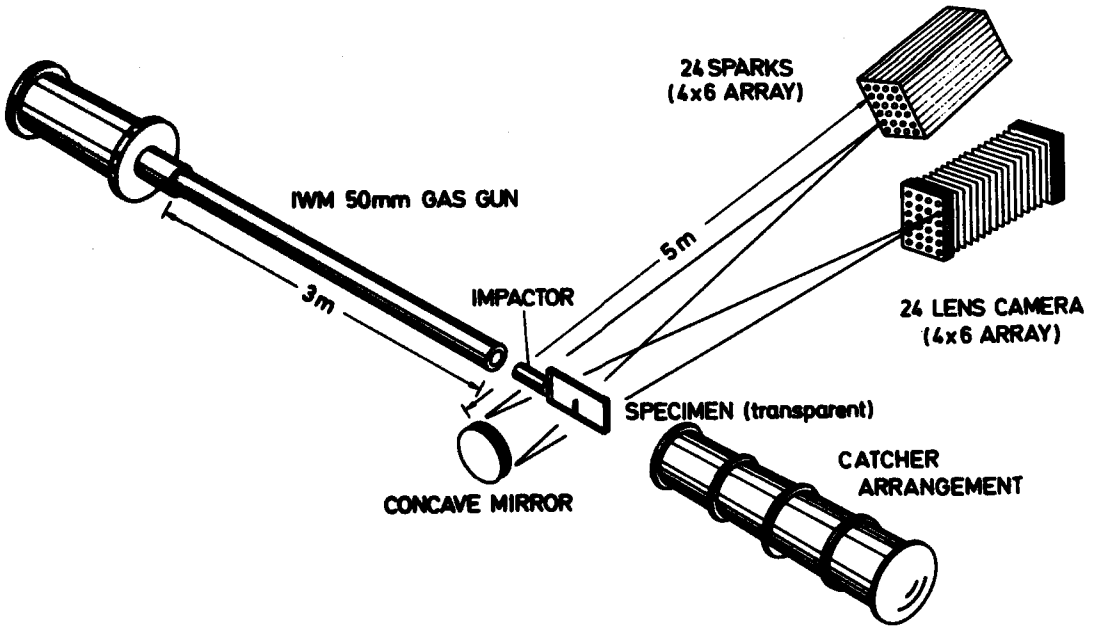

Fig. 4 Experimental set-up, schematically

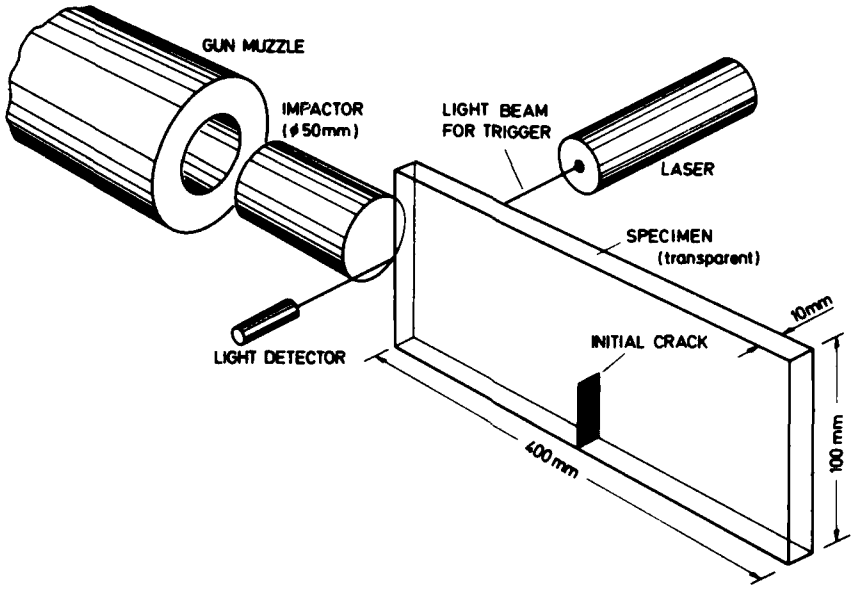

Fig. 5 Illustrative view of the direct impact loading arrangement

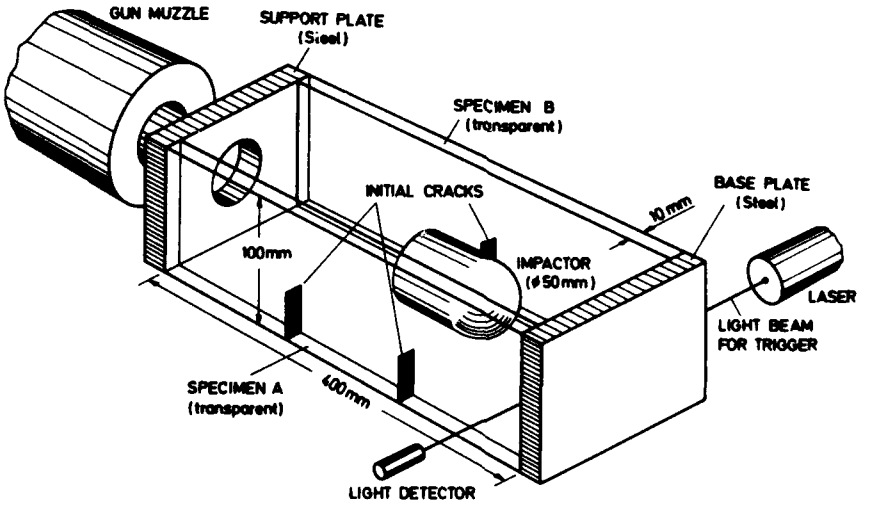

Fig. 6 Illustrative view of the base plate loading arrangement

2.2 The Shadow Optical Method of Caustics

The method of caustics is an optical tool for measuring stress intensifications. The technique has been introduced by Manogg in 1964 [30,31]. Later on, Theocaris [32] further developed the method. The authors and their coworkers extended and applied Manoggs technique for investigating dynamic fracture phenomena [4, 33-39].

The physical principle of the method is illustrated in Fig. 7. A precracked specimen under load is illuminated by a parallel light beam. A cross-section through the specimen at the crack tip is shown in Fig. 7b for a transparent specimen, and in Fig. 7c for a non-transparent steel specimen. Due to the stress concentration the physical conditions at the crack tip are changed. For transparent specimens both the thickness of the specimen and the refractive index of the material are reduced. Thus, the area surrounding the crack tip acts as a divergent lens and the light rays are deflected outwards. As a consequence, on a screen (image plane) at a distance z_0 behind the specimen a shadow area is observed which is surrounded by a region of light concentration, the caustic (see Fig. 8). Fig. 7c shows the situation for a non-transparent steel specimen with a mirrored front surface. Due to the surface deformations light rays near the crack tip are reflected towards the center line. An extension of the reflected light rays onto a virtual image plane at the distance z_0 behind the specimen results in a light configuration which is similar to the one obtained in transmission. Consequently a similar caustic is obtained. The mode I shadow pattern was calculated by Manogg [31] from the linear elastic stress strain field around the crack tip. Fig. 8 compares theoretical results with experimentally observed caustics which were photographed in transmission and in reflection with different materials. The single caustic curve obtained for isotropic materials splits up into a double caustic for optically anisotropic materials.

The size of the shadow pattern is related to the stress intensification at the crack tip. The quantitative correlation between the diameter D of the caustic and the stress intensity factor K_I is given by the equation

$$K_I = M \cdot D^{5/2} \qquad (1)$$

where M is a known numerical factor which depends on the optical arrangement and the material utilized [33, 34].

A quantitative shadow-optical analysis is also available for cracks subjected to superimposed tensile (mode I) and shear (mode II) loading. With increasing ratio $\mu = K_{II}/K_I$ the caustic becomes asymmetrical (see Fig. 9a). Fig. 9b shows the theoretically calculated caustic in comparison to an experimentally observed shadow pattern for the case $\mu = 1$. From the minimum and maximum diameters D_{min} and D_{max} of the caustics (defined in Fig. 9b) the absolute values of the stress intensity factors K_I and K_{II} can be determined using the relation

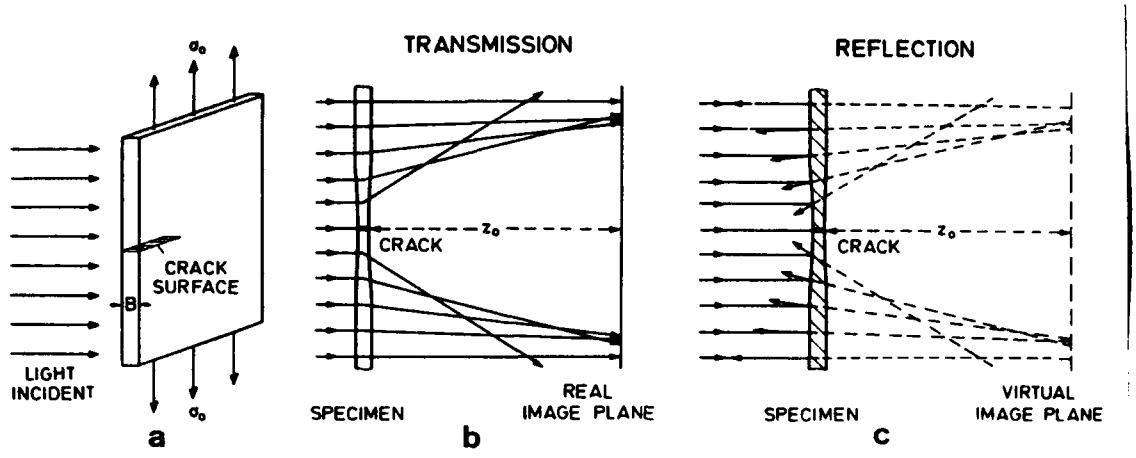

Fig. 7 Physical principles of the shadow optical method of caustics

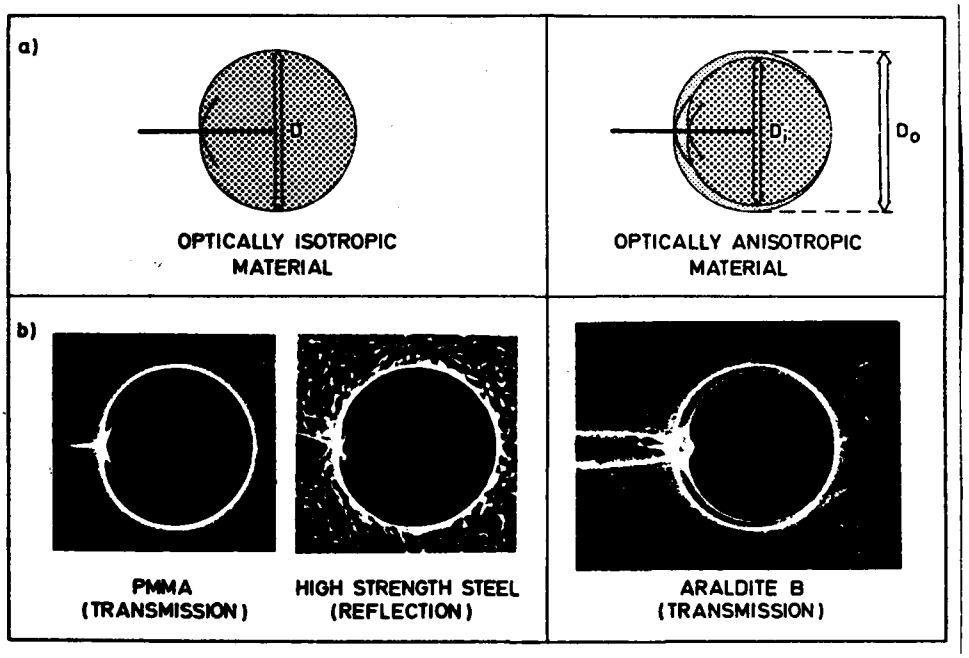

Fig. 8 Mode-I caustics, a) calculated, b) measured

$$K_i = M_{i,k} \cdot D_k^{5/2} \qquad (i = I,II;\ k = min,\ max). \qquad (2)$$

This relation is similar to eq.(1). The (four possible) factors $M_{i,k}$ which again contain optical and geometrical parameters are known functions [39-41].

For further details of the shadow optical techniques see [33,34,42]. Crack tip caustics are of a simple form and can easily be evaluated. The technique, therefore, is very well suited for investigating complex phenomena, as e.g. in fracture dynamics, and is used in this work to measure dynamic stress intensity factors under impact loading.

2.3 Research Program

Within the first year of a three year's research project the experimental set-up for investigating the fracture behavior under impact loading has been built up. The existing IWM gas gun has been modified for this purpose. A Cranz Schardin high speed camera has been aligned to the gas gun. A holding fixture has been designed and built to load the specimens under direct impact - and base plate loading conditions. The set-up has been succesfully tested under different impact conditions. Several series of experiments have been performed to specify the parameters for the main investigations. For the second year, i.e. this reporting period, main experiments with a systematic variation of parameters were scheduled. In particular, the impact fracture toughness K_{Id} should be measured at different loading rates. In addition, the mutual interaction of multiple crack configurations should be studied. It was planned to carry out these investigations predominently with Araldite B specimens. For the third year investigations with high strength steel specimens are scheduled.

3 DEPENDENCE OF IMPACT FRACTURE TOUGHNESS ON LOADING RATE

Experiments have been performed to investigate the dependence of the impact fracture toughness K_{Id} on loading rate. Most impact fracture data reported so far have been measured at modest loading rates under drop weight loading or in a pendulum type impact tester. Under these loading conditions the impact fracture toughness in general decreases with increasing loading rate, as already shown in Fig. 3. Experiments at higher loading rates allow to discriminate between the following behavior: a) a continuous decrease of the impact fracture toughness with increasing loading rate to zero values, b) the existence of a minimum fracture toughness which cannot be undergone even if the loading rate is increased, or c) a decrease of toughness followed by a final increase at very high loading rates. These different possibilities of the impact fracture toughness behavior are shown in the schematic representation of Fig. 10. Within this research project impact fracture data at higher loading rates than under drop weight loading are generated applying the two different techniques of directly impacting the specimen by a projectile or by loading the specimen in the base plate test arrangement.

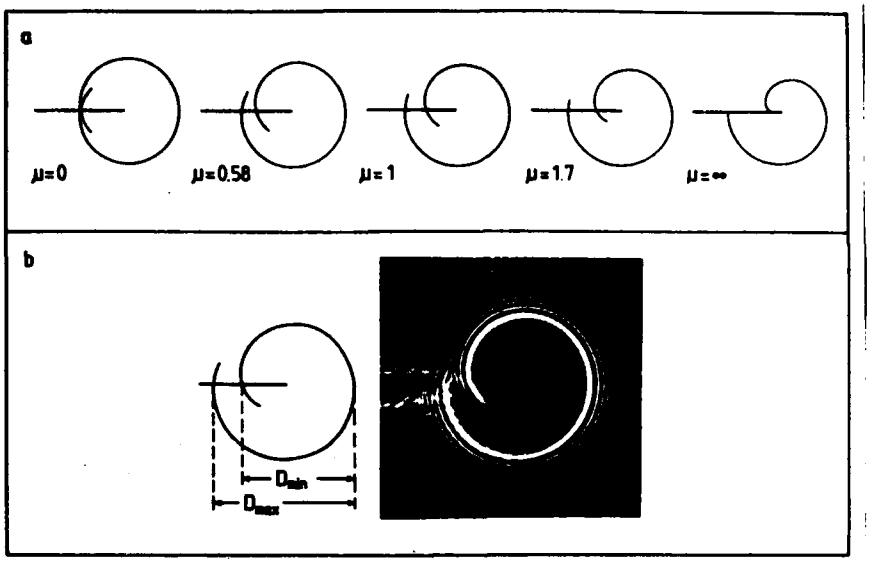

Fig. 9 Mixed (I,II) mode caustics, a) calculated for different ratios $\mu = K_{II}/K_I$, b) definition of diameters and experimentally observed shadow pattern

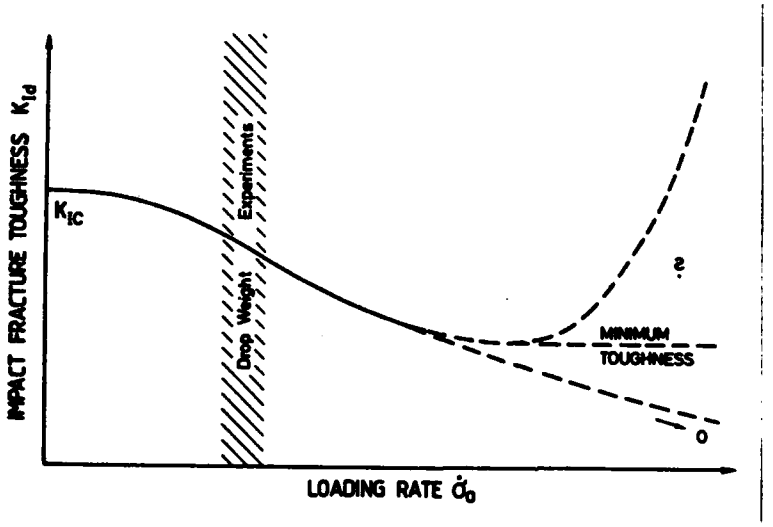

Fig. 10 Dependence of the impact fracture toughness on loading rate

3.1 Results of Base Plate Loading Experiments

Precracked specimens made from the model material Araldite B have been dynamically loaded in the base plate loading arrangement (see Fig. 6). Details of the experimental procedure have been reported in the First Annual Report [43]. Some data that are necessary for the following presentation of results shall be repeated here: The specimen dimensions were 400 x 100 x 10 mm^3. The specimens were precracked by a single edge crack. The crack length has been varied from 20 mm to 50 mm. Due to symmetry reasons two specimens were simultaneously tested in each experiment. In order to allow for an undisturbed observation of each individual caustic the cracks of length less then 50 mm (i.e. half the specimen width) were inserted from opposite edges of the specimens. In the case of specimens with a crack of length >50 mm a specimen with a double crack configuration has been used as the second test specimen. The results obtained from the double crack configuration are presented in Chapter 4 "Dynamic Interaction of Multiple Cracks".

The two specimens are fastened at one end to the base plate (100 x 100 x 20 mm^3) made from a hardened steel (1,6 kg mass). The other ends are fastened to the muzzle of the gas gun. The base plate is accelerated by an impinging steel projectile of 50 mm diameter. Projectiles of different lengths, i.e. different masses, have been utilized in the experiments: 50 mm, 75 mm and 140 mm. The impact velocity has been varied from about 10 m/s to 40 m/s.

Typical results are shown in Figs. 11 and 12 (see also First Annual Report [43]). Fig. 11 shows a series of shadow optical photographs. It shall be emphasized that these pictures do not show one specimen with a configuration of three cracks but two specimens, one with a single crack (i.e. the middle crack in the photographs) and one with a double crack configuration (i.e. the outer cracks in the photographs). The tensile stress pulse impinges on the cracks from the left side. Only the behavior of the center crack, i.e. the single edge crack, is discussed here. In the first pictures the stress intensity factor increases with time. Between pictures No. 12 and No. 13, i.e. at ~135 µs, the crack becomes unstable and propagates through the specimen (last two pictures).

Quantitative data are shown in Fig. 12. The dynamic stress intensity factor, K_I^{dyn}, and the momentary crack length, a, are plotted as functions of time. The a(t)-data give an indication of the time at which the crack becomes unstable. With this information the interesting fracture parameters can be determined: The critical stress intensity factor for onset of rapid crack propagation, i.e. the dynamic fracture toughness K_{Id}; the time to fracture t_f; and the effective stress intensification rate $\dot{K}_I^{dyn}$.

About 60 experiments have been performed. Several experiments failed due to experimental difficulties. A complete series of experiments showing very large uncontrolled scatter in the data had to be rejected since

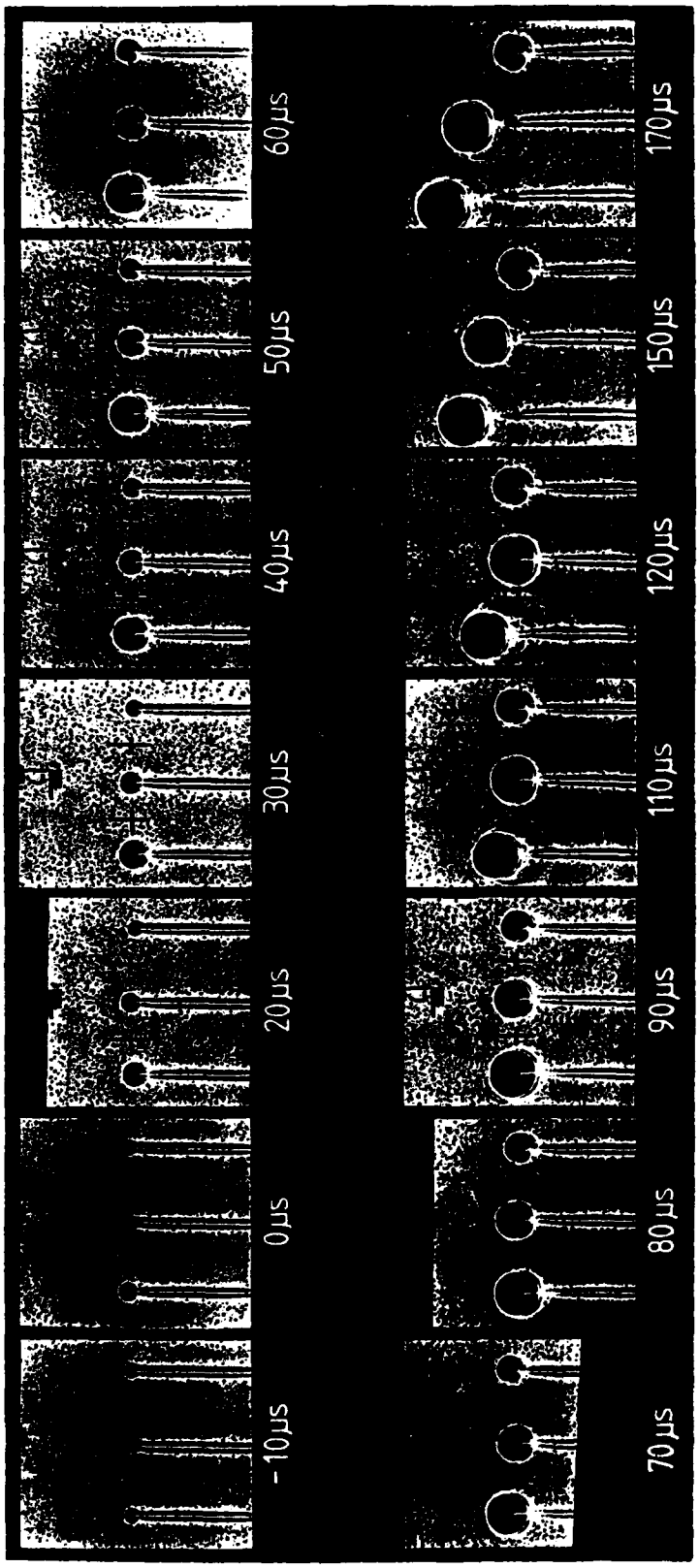

Fig. 11 Crack tip caustics, a single (inner) crack and a double crack configuration (outer cracks) under base plate loading

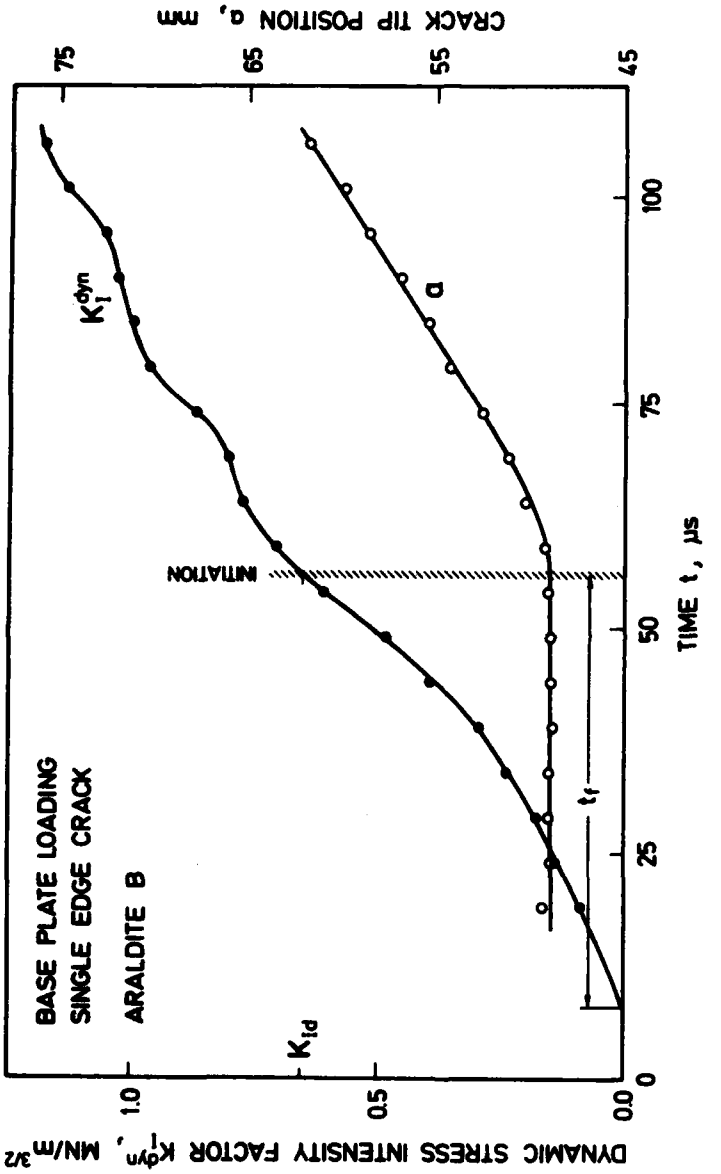

Fig. 12 Dynamic stress intensity factor and crack tip position, base plate loading

heavy work was simultaneously going on in the laboratory due to moving of heavy test equipment from one institute building into another. Data of successful experiments are summarized in Table 1. Presented are the specimen and projectile dimensions, the impact velocity, and data on the crack instability behavior, i.e. the time to fracture t_f and the impact fracture toughness K_{Id}. When specimens with double crack configurations were simultaneously tested these data are given here as well for completeness.

In Figs. 13 and 14 the obtained times to fracture t_f and the stress intensification rates $\dot{K}_I^{dyn}$ are plotted as functions of the impact velocity v_0. Most of the data were obtained from shots with projectiles of 75 mm length, i.e. 1 kg mass. Only some experiments have been performed with projectiles of different masses: 2 kg (140 mm length) and 0.5 kg (50 mm length). In accordance with expectations the time to fracture becomes smaller with increasing impact velocity and the stress intensification rate $\dot{K}_I^{dyn}$ accordingly increases with increasing impact velocity. The scatter of the data is still rather high (see First Annual Report [43], p. 37), in particular for the stress intensification rate. Changes in the results due to variations in the mass of the projectile are not significant. It is speculated that the large scatter is due to still existing slight variations in the process of how the specimens are fastened to the base plate.

In Figs. 15 and 16 the impact fracture toughness values K_{Id} are plotted as functions of the impact velocity v_0 and the time to fracture t_f. The data show a scatter of about 10 to 20%, which is usual for toughness testing. Within the range of achieved loading rates the K_{Id} data do not vary. In Figs. 15 and 16 the data scatter around the value of 0.67 $MN/m^{3/2}$, which is almost the same as the static fracture toughness value $K_{Ic} = 0.7$ $MN/m^{3/2}$. In Fig. 17 the impact fracture toughness data are plotted as a function of the kinetic energy of the projectile, $1/2\ m \cdot v_0^2$, were m is the mass of the projectile. As in the previous two diagrams a dependence of the impact fracture toughness is not observed.

It is speculated that the observation of constant fracture toughness data as a function of loading rate is due to two facts: First, Araldite B is a very brittle material and loading rate effects will have only little influence on the material behavior. Secondly, the times to fracture achieved in the experiments were still rather large, i.e. the maximum obtained loading rate was only modest.

3.2 Results of Direct Impact Loading Experiments

Similar specimens as tested in the base plate loading arrangement have been directly impacted by a projectile. As in the investigations discussed before the specimens were made from Araldite B, the dimensions were 400 x 100 x 10 mm^3. The length of the initial cracks was varied from 12 mm to 40 mm. Projectiles of 50 mm diameter and 200 mm length machined from Araldite B were utilized in these experiments. For further

Spec. No.	Crack Length a_o, mm	Crack Tip	Projectile			Time to Fracture t_f, μs	Impact Fracture Toughness K_{Id}, $MN/m^{3/2}$
			m, kg	l, mm	v_o, m/s		
623	34.0	s	0.48	200	25.9	11.0	0.562
655	25.0	s	0.48	200	8.6	18.5	0.730
656	25.0	s	0.48	200	11.7	-	-
657	25.0	s	0.48	200	10.5	21.0	0.670
658	25.0	s	0.48	200	10.6	20.0	0.690
659	31.5	s	0.48	200	9.8	11.2	0.710
660	32.0	s	0.48	200	11.4	20.0	0.690
661	32.0	s	0.48	200	11.4	14.2	0.670
662	40.0	s	0.48	200	11.8	-	0.680
663	40.0	s	0.48	200	10.9	-	0.660
664	12.0	s	0.48	200	13.0	-	0.670
665	12.5	s	0.48	200	13.0	-	-
666	12.0	s	0.48	200	13.3	-	-
667	12.5	s	0.48	200	11.9	12.5	0.670

s = sharp, b = blunted

Table 1 Test conditions and results of base plate loading experiments, single edge cracks

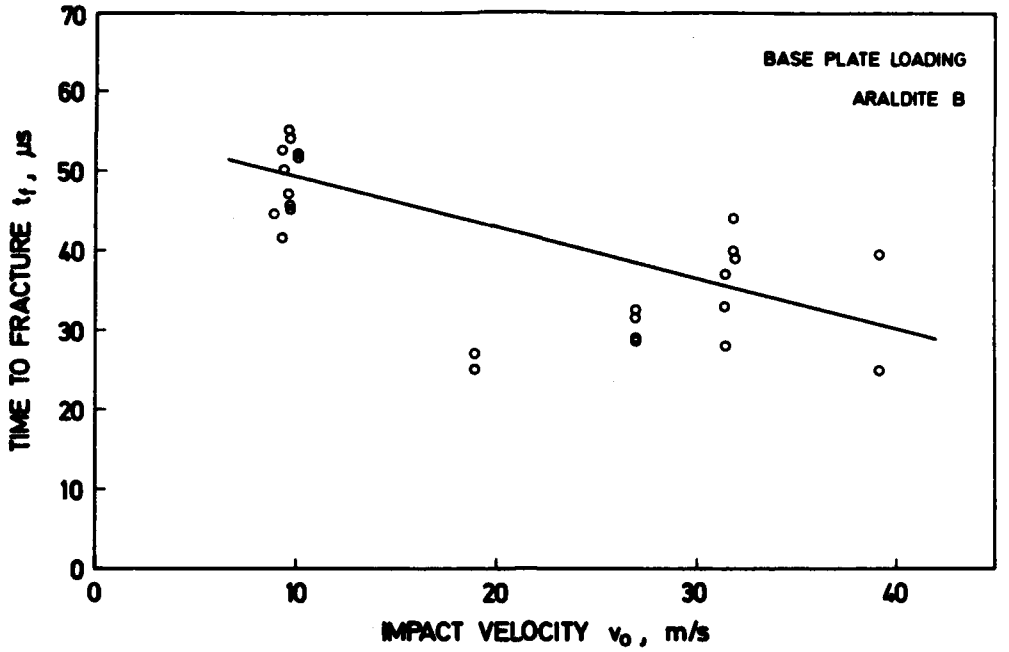

Fig. 13 Time to fracture versus impact velocity

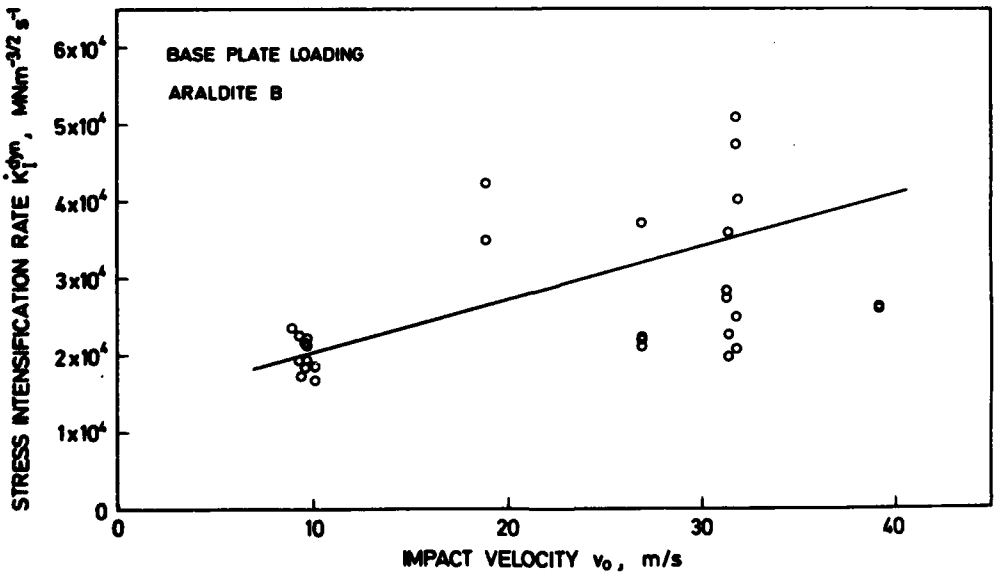

Fig. 14 Stress intensification rate versus impact velocity

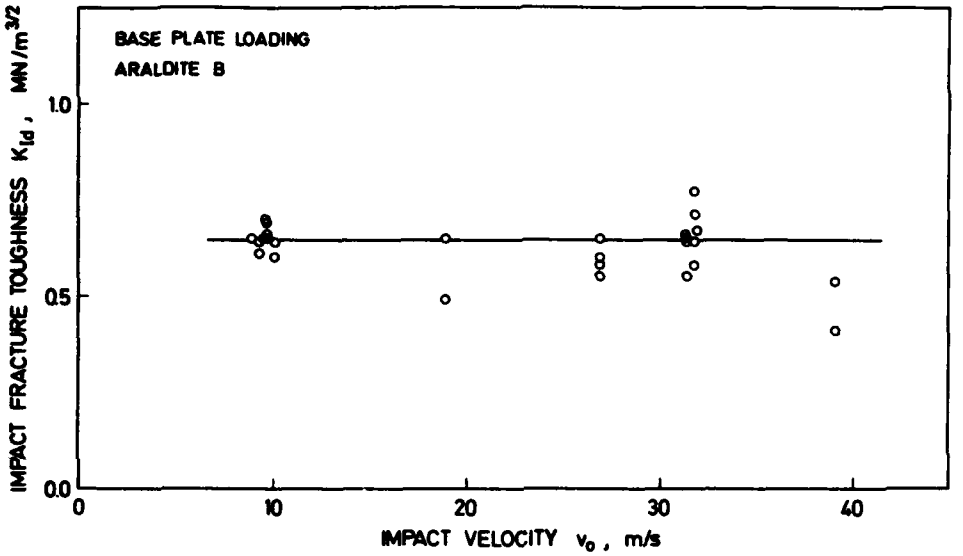

Fig. 15 Impact fracture toughness versus impact velocity

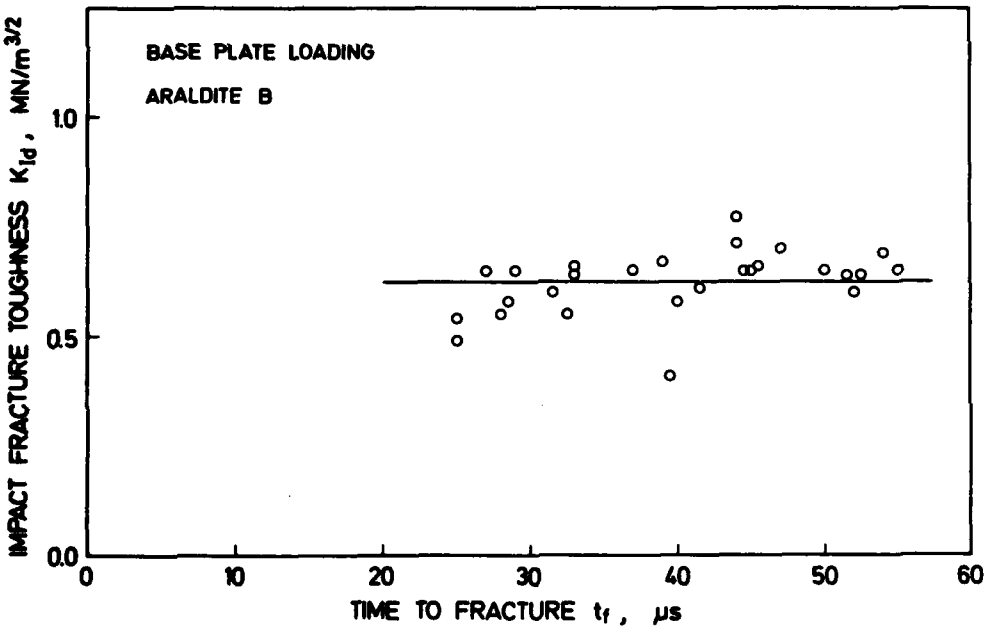

Fig. 16 Impact fracture toughness versus time to fracture

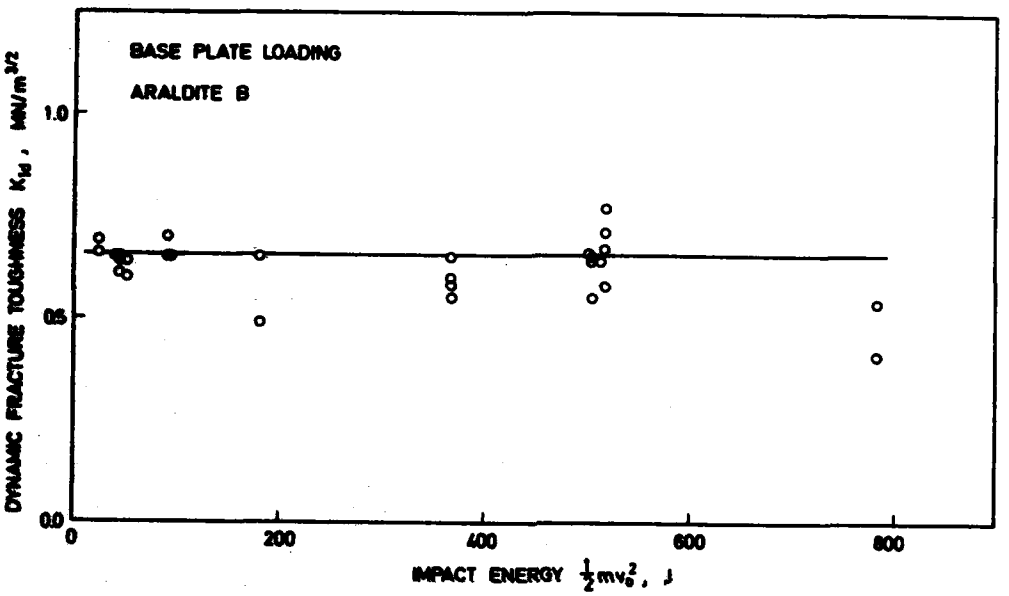

Fig. 17 Impact fracture toughness versus impact energy

details of the experimental procedure see the First Annual Report [43]. The impact velocity in most of the experiments performed so far was about 10 m/s, a few experiments have been carried out at higher velocities.

The results of a typical experiment are shown in Figs. 18 and 19. In Fig. 18 twelve of a series of 24 shadow optical pictures are reproduced. The pictures No. 1 to 4 show the increase of the dynamic stress intensity factor at the tip of the stationary crack. At picture No. 5 the crack has become unstable. Pictures No. 6 to 12 show the propagating crack. In Fig. 19 quantitative data are given which were obtained according to eq. (1) from the shadow optical photographs. The dynamic stress intensity factor, K_I^{dyn}, and the momentary position of the crack tip, a, are plotted as functions of time. Similar as under base plate loading conditions the properties K_{Id}, t_f, and $\dot{K}_I^{dyn}$ can be obtained from these plots.

About 70 experiments total have been performed. The results of successful experiments which have been utilized in the following graphs are summarized in Table 2.

In Figs. 20 and 21 the obtained times to fracture t_f and the stress intensification rates $\dot{K}_I^{dyn}$ are plotted as a function of the impact velocity v_0 (full data points). For comparison the equivalent data obtained under base plate loading conditions (open data points) are shown in the same diagram. In accordance with expectations the times to fracture become smaller and the stress intensification rates are higher than for base plate loading conditions. The differences in loading rates are about a factor of 3.

Fig. 22 shows the impact fracture toughness data K_{Id} as a function of the time to fracture (full data points) together with the data for the base plate loading experiments (open data points). The data from the direct impact experiments supplement the base plate data into the lower time to fracture regime. All data, however, fall within the same scatter band. One might argue that the direct impact data lie at the upper boundary of the scatter band observed for the base plate loading experiments. It would be premature, however, to derive definite conclusions from this trend in the data.

A strong increase of the fracture toughness with increasing loading rate, i.e. with decreasing time to fracture, was observed by Ravi Chandar and Knauss [44] with Homalite-100 specimens loaded by electromagnetic techniques (see Fig. 23). Kalthoff et al. [38, 45] speculate that such a behavior can be explained by assuming the existence of an incubation time: According to this assumption (see Fig. 24) the crack tip would have to experience a supercritical stress intensity factor $K_I > K_{I,crit}$ for a constant (very likely material related) minimum time, i.e. the incubation time, before onset of rapid crack propagation can occur. If the stress intensification $\dot{K}_I^{dyn}$ increases slowly with time the critical stress intensity factor for onset of rapid crack pro-

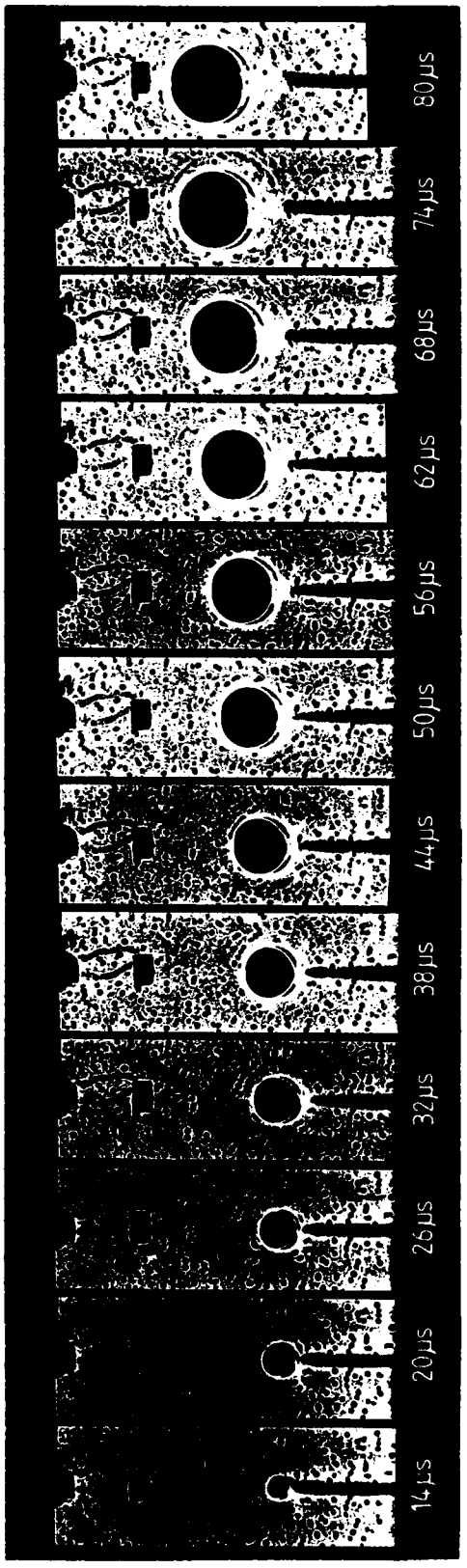

Fig. 18 Crack tip caustics, single crack under direct impact loading

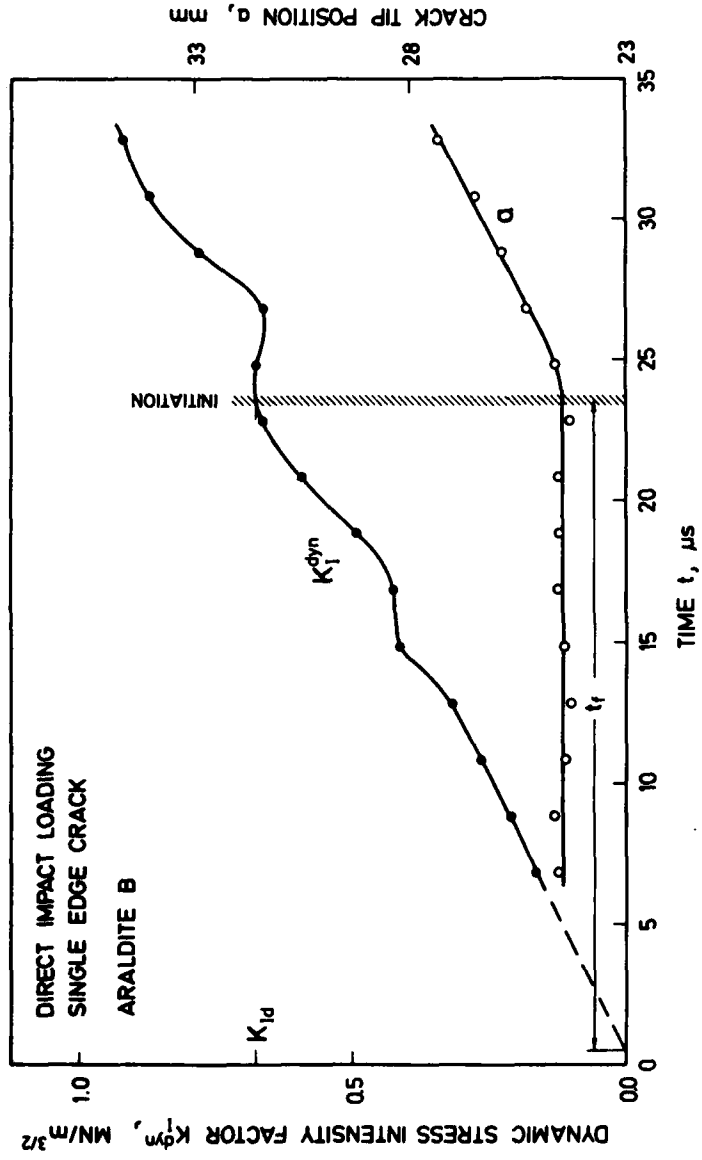

Fig. 19 Dynamic stress intensity factor and crack tip position, direct impact loading

Spec. No.	Crack Length a_o, mm	Crack Distance d, mm	Crack Tip	Projectile m, kg	Projectile l, mm	Projectile v_o, m/s	Time to Fracture t_f, μs	Impact Fracture Toughness K_{Id}, $MN/m^{3/2}$
670	50	0	b	1.02	75	10.7	-	-)
(670	50	60	b	1.02	75	10.7	-	-
674	50	0	b	1.02	75	10.1	-	-
(674	50	60	b	1.02	75	10.1	-	-)
677	50	0	s	2.01	139	9.6	-	0.664
(677	50	60	s	2.01	139	9.6	-	0.640)
687	50	0	s	1.02	74	9.9	-	-
(687	50	60	s	1.02	74	9.9	-	-)
688	50	0	s	1.02	74	10.1	52.0	0.600
(688	50	60	s	1.02	74	10.1	51.5	0.640)
689	50	0	s	1.02	74	9.3	52.5	0.640
(689	50	60	s	1.02	74	9.3	41.5	0.610)
690	50	0	s	1.02	74	8.9	-	-
(690	50	60	s	1.02	74	8.9	44.5	0.650)
691	50	0	s	1.02	74	31.9	39.0	0.670
(691	50	60	s	1.02	74	31.9	-	-)
692	40	0	s	1.02	74	9.4	38.0	0.650
692	40.5	0	s	1.02	74	9.4	-	-
693	40	0	s	1.02	74	9.4	-	-
693	40.5	0	s	1.02	74	9.4	12.5	0.640
694	40	0	s	1.02	78	31.9	-	-
694	40.5	0	s	1.02	78	31.9	-	-
695	40	0	s	1.02	78	31.8	-	-
695	40	0	s	1.02	78	31.8	16.0	0.770
696	40	0	s	1.02	78	31.4	-	-
696	40.5	0	s	1.02	78	31.4	17.8	0.650
697	40	0	s	1.02	78	31.4	32.3	0.640
697	40	0	s	1.02	78	31.4	24.3	0.505
698	40.5	0	s	1.02	78	31.8	28.3	0.580
698	40.5	0	s	1.02	78	31.8	28.8	0.710
699	30	0	s	1.02	78	31.3	23.5	0.660
699	30	0	s	1.02	78	31.3		

700	30	0	s	1.02	78	39.1	27.0	-
700	30	0	s	1.02	78	39.1	18.0	-
701	50	0	s	1.02	78	18.9	25.0	0.490
(701	50	60	s	1.02	78	18.9	27.0	0.650)
702	50	0	s	1.02	78	26.9	28.5	0.580
(702	50	60	s	1.02	78	26.9	31.5	0.600)
703	50	0	s	1.02	78	26.9	32.5	0.550
(703	50	60	s	1.02	78	26.9	29.0	0.650)
705	50	0	s	1.98	142	9.7	-	-
(705	50	60	s	1.98	142	9.7	45.0	0.650)
706	50	0	s	1.98	142	9.6	55.0	0.650
(706	50	60	s	1.98	142	9.6	47.0	0.700)
707	50	0	s	0.51	50	9.7	54.0	0.690
(707	50	60	s	0.51	50	9.7	45.5	0.660)
717	15	0	b	1.02	78	9.2	-	-
(717	15	20	b	1.02	78	9.2	-	-)

s = sharp, b = blunted

Table 2 Test conditions and results of direct impact loading experiments, single edge cracks

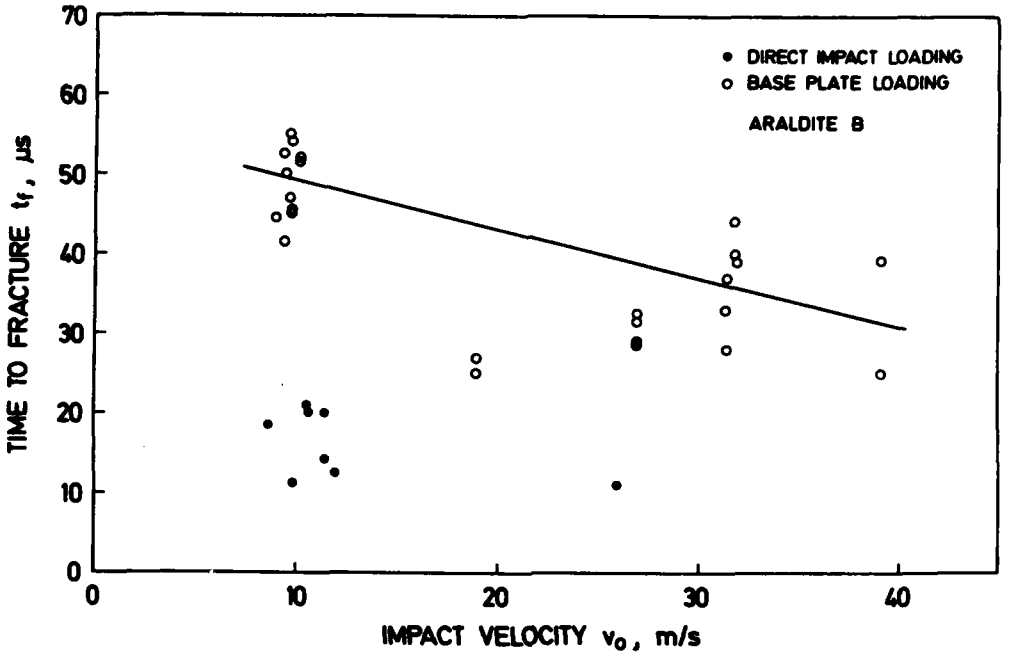

Fig. 20 Times to fracture versus impact velocity

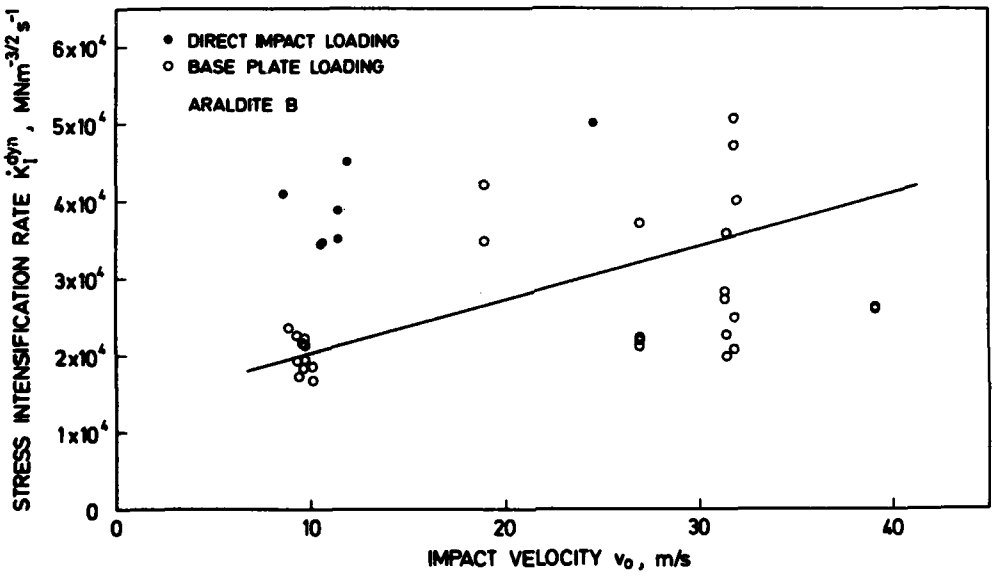

Fig. 21 Stress intensification rates versus impact velocity

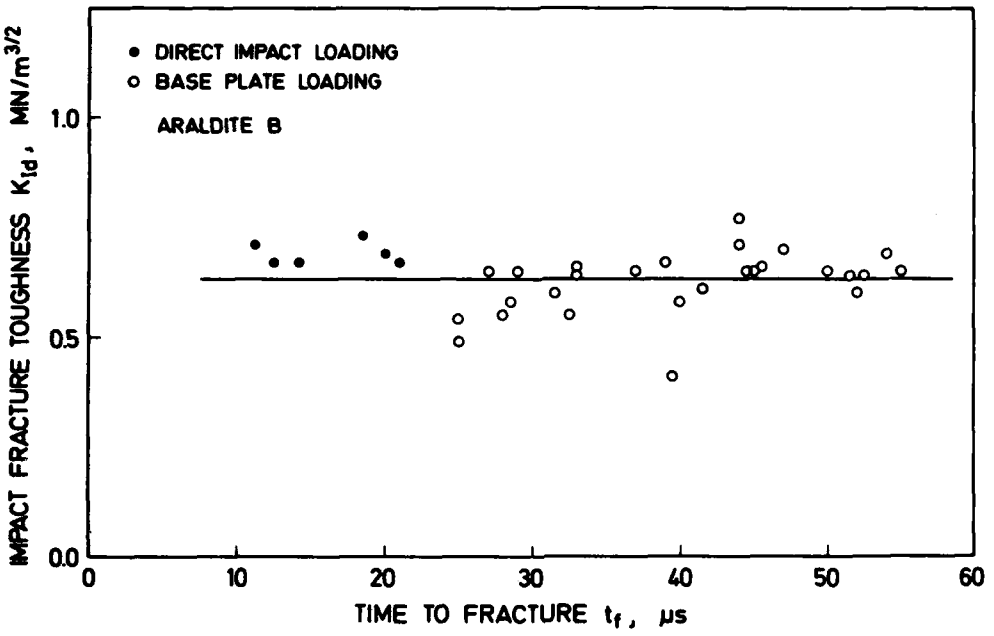

Fig. 22 Impact fracture toughness versus time to fracture

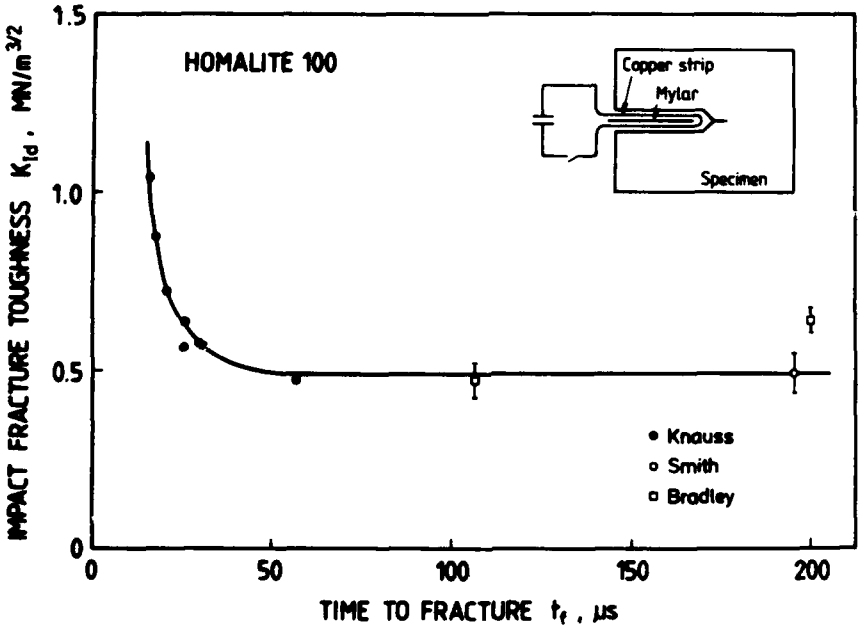

Fig. 23 Dependence of impact fracture toughness on time to fracture (after Ravi Chandar, Knauss [44])

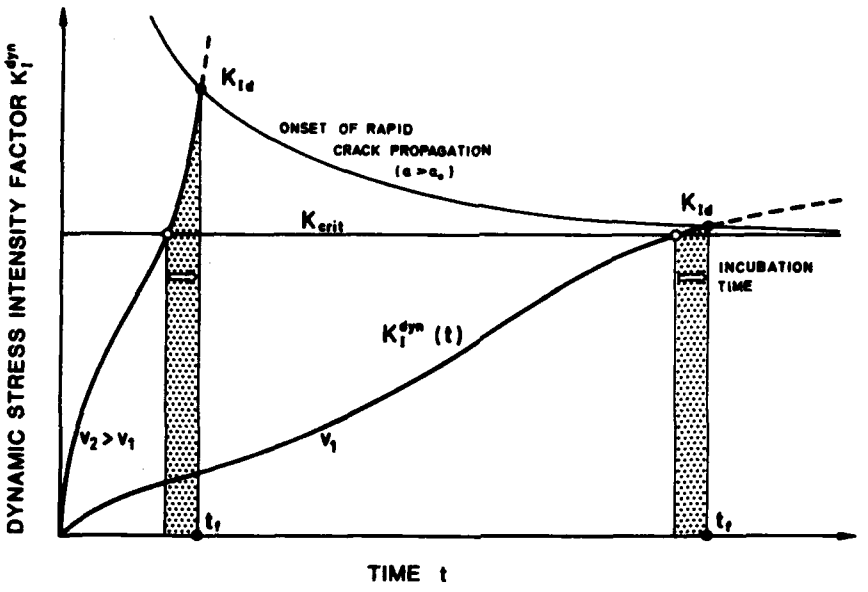

Fig. 24 Influence of incubation time on the impact fracture toughness

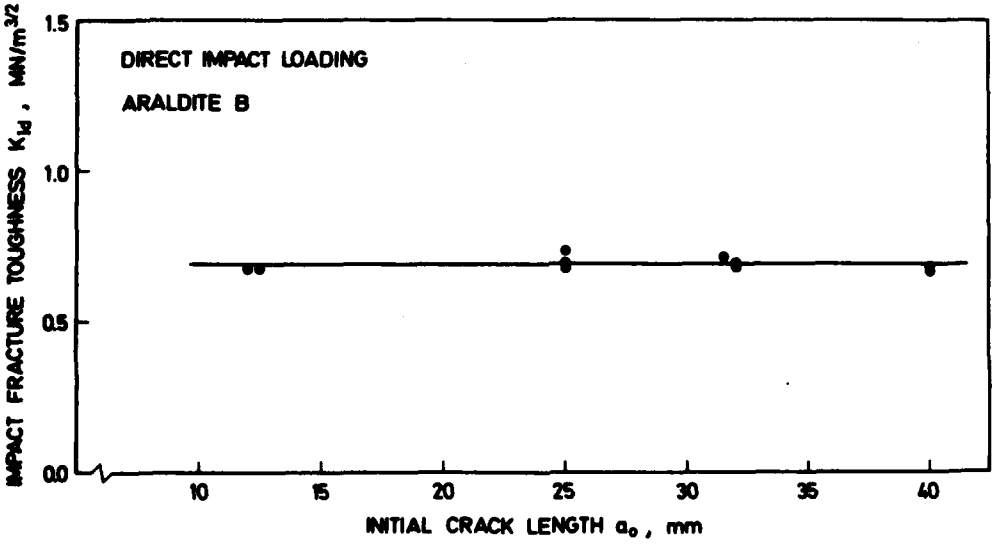

Fig. 25 Impact fracture toughness versus crack length

pagating K_{Id} would be practically the same as the critical stress intensity factor $K_{I\,crit}$. But, if the slope of the $K_I^{dyn}(t)$-curve is very steep the increase of the stress intensity factor within the incubation time can be very large, and consequently $K_{Id} > K_{I\,crit}$. Further data at higher loading rates are necessary to support this speculation.

Since it might also be possible that not the absolute time to fracture, t_f, but the ratio of the time to fracture to the crack length, t_f/a_o, influences the instability event the crack length has been varied in the experiments. Fig. 25 shows the measured impact fracture toughness data as a function of crack length. In Fig. 26 all data (obtained under base plate - and under direct impact loading) are plotted as a function of the dimensionless time $(c_1/a_o)t$, where c_1 is the longitudinal wave velocity. Also this plot does not show any trend in the data but a constant behavior.

For the next reporting period further experiments at higher loading rates are planned: Araldite B specimens under direct loading conditions will be impacted at velocities up to 40 m/s in order to supplement the presented data into the lower time to fracture regime. Furthermore, following the original research program, experiments will be performed utilizing high strength steel specimens. The steel specimens will be tested at velocities which can be higher than the maximum allowable velocity of 40 m/s for Araldite B specimens. Since steel is more strain rate sensitive than Araldite B and since the impact velocities will be considerable higher more informative results are expected.

4 DYNAMIC INTERACTION OF MULTIPLE CRACKS

The fracture behavior of a structure which contains a configuration of multiple cracks is different from the one with only one crack: The stress fields of multiple cracks have a mutual influence on each other. Due to this interaction the stress intensity factors K_I^{dbl} of two parallel cracks under static loading condition are smaller than the stress intensity factor K_I^{sgl} for an equivalent single crack; in addition a superimposed mode-II loading results. This is illustrated in Fig. 27. If the multiple crack configuration is hit by a tensile stress pulse the stress intensifications at the crack tips will become complicated functions of time. The experiments reported in this Chapter are aimed to study in detail the influences which control the interaction processes.

The base plate loading arrangement has been utilized to test specimens with double crack configurations. The cracks are oriented perpendicular to the impinging stress pulse. The test conditions were the same as reported in Chapter 3.1 "Results of Base Plate Loading Experiments". The crack length was varied from 15 mm to 50 mm, the distance of the two cracks was varied from 20 mm to 80 mm. The length of the two cracks in each experiment has been kept the same. The impact velocity has been varied from about 10 m/s to 30 m/s. Since it has not been the goal of these experiments to investigate the instability event, but the mutual

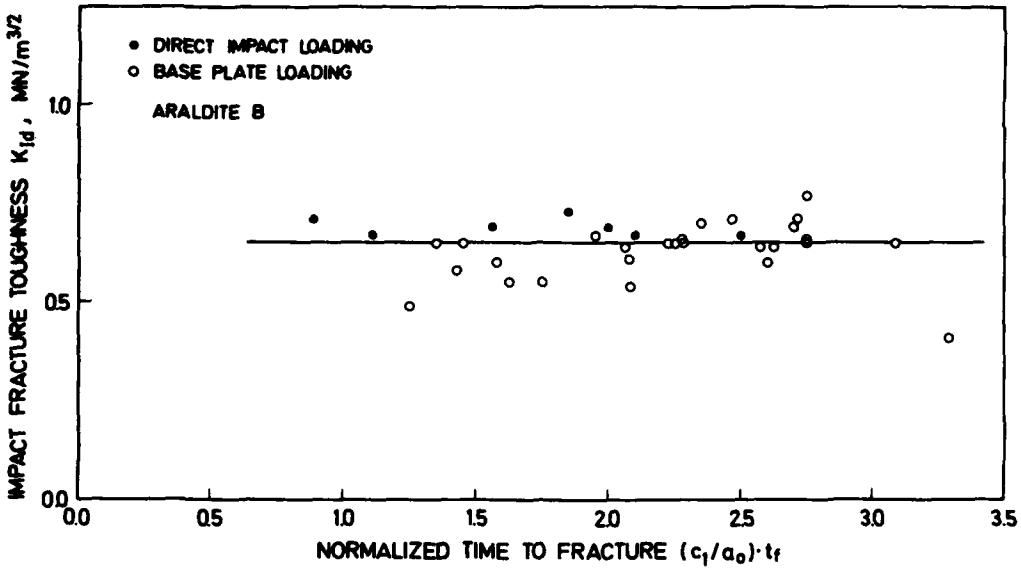

Fig. 26 Impact fracture toughness versus normalized time to fracture

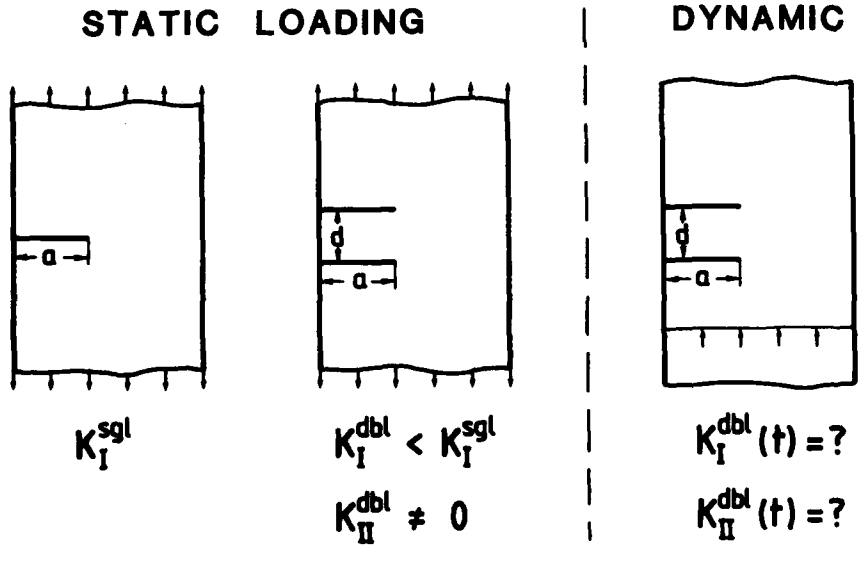

Fig. 27 Mutual interaction of multiple cracks, schematically

interaction of the cracks as a function of time, blunted notches instead of sharp initial cracks have been utilized in these experiments. Thus, crack initiation was delayed and the interaction processes could be observed over longer time ranges. An overview on the test conditions of the successful experiments is given in Table 3.

A typical series of shadow optical photographs has already been shown in Fig. 11. The outer cracks represent the double crack configuration in one of the two specimens. These are the data which are of interest in this context. The center crack is the single crack in the other specimen (these data have been discussed already in Chapter 3.1 and are not considered here). The crack configuration is hit by a tensile stress pulse from the left side. The left hand crack is loaded the longest time and exhibits the largest stress intensity factor. The shadow pattern of the left hand crack is of mode-I type, at least for early times. The shadow pattern of the right hand crack is of mixed mode type from the very beginning on, since this crack is always influenced by the stress field of the left hand crack. In the picture No. 11, at 110 µs, the left hand crack becomes unstable and propagates through the specimen. The path shows a slight deviation from the original direction indicating a slight superimposed mode-II loading also for this crack at larger times. For convenience the crack which is hit first by the stress pulse is denoted "crack A", the second crack which is hit afterwards is denoted "crack B".

Fig. 28 shows results for cracks of 50 mm length with distances d = 20 mm, 40 mm, and 80 mm. In this Figure only the mode I stress intensity factors for both cracks are plotted as functions of time. The following behavior is deduced from these results: the cracks A exhibit the largest stress intensity factors and these stress intensity factors build up earlier than for cracks B, since cracks A are hit first. The time shift between the $K_I^{dyn}(t)$-curves for cracks A and cracks B increases with the distance d between the two cracks. The time shifts, however, are larger than one would expect due to a simple consideration of wave propagation times. Till about 60 µs the $K_I^{dyn}(t)$-curves for the cracks A are the same, regardless of the distance between the two cracks A and B. Obviously the cracks A behave similar as a single crack and are not disturbed much by cracks B. For the narrow crack configuration (d = 20 mm) the interaction with crack B than leads to a reduction of the crack A stress intensity factor for times larger than 60 µs. The crack A stress intensity factors for wider crack configurations (d = 40 and 80 mm) still follow the same curve exhibiting a rather undisturbed single crack behavior.

The results for mode-II stress intensity factors of the experiments under consideration are shown in Fig. 29. For two crack configurations, d = 20 mm and 80 mm, the mode-II stress intensity factors are plotted as functions of time *). Data of other experiments have been omitted for

*) The time scale relates to the one in Fig. 28

Spec. No.	Crack Length a_o, mm	Crack Distance d, mm	Crack Tip	Projectile			Time to Fracture t_f, μs	Impact Fracture Toughness K_{Id}, $MN/m^{3/2}$
				m, kg	l, mm	v_o, m/s		
670	50	60	b	1.02	75	10.7	-	-
(670	50	0	b	1.02	75	10.7	-	-)
674	50	60	b	1.02	75	10.1	-	-
(674	50	0	b	1.02	75	10.1	-	-)
677	50	60	s	2.01	139	9.6	-	0.640
(677	50	0	s	2.01	139	9.6	-	0.660)
687	50	60	s	1.02	74	9.9	-	-
(687	50	0	s	1.02	74	9.9	-	-)
688	50	60	s	1.02	74	10.1	51.5	0.640
(688	50	0	s	1.02	74	10.1	52.0	0.600)
689	50	60	s	1.02	74	9.3	41.5	0.610
(689	50	0	s	1.02	74	9.3	52.5	0.640)
690	50	60	s	1.02	74	8.9	44.5	0.650
(690	50	0	s	1.02	74	8.9	-	-)
691	50	60	s	1.02	74	31.9	-	-
(691	50	0	s	1.02	74	31.9	39.0	0.670)
701	50	60	s	1.02	78	18.9	27.0	0.650
(701	50	0	s	1.02	78	18.9	25.0	0.490)
702	50	60	s	1.02	78	26.9	31.5	0.600
(702	50	0	s	1.02	78	26.9	28.5	0.580)
703	50	60	s	1.02	78	26.9	29.0	0.650
(703	50	0	s	1.02	78	26.9	32.5	0.550)
705	50	60	s	1.98	142	9.7	45.0	0.650
(705	50	0	s	1.98	142	9.7	-	-)
706	50	60	s	1.98	142	9.6	47.0	0.700
(706	50	0	s	1.98	142	9.6	55.0	0.650)
707	50	60	s	0.51	50	9.7	45.5	0.660
(707	50	0	s	0.51	50	9.7	54.0	0.690)
709	50	80	b	1.02	78	9.0	-	-
709	50	20	b	1.02	78	9.0	-	-

710	50	40	b	1.02	78	10.3	-	-
710	25	20	b	1.02	78	10.3	-	-
711	50	20	b	1.02	78	10.3	-	-
711	25	20	b	1.02	78	10.3	-	-
713	15	20	b	1.02	78	9.5	-	-
713	25	20	b	1.02	78	9.5	-	-
715	15	20	b	1.02	78	10.8	-	-
715	15	20	b	1.02	78	10.8	-	-
717	15	20	b	1.02	78	9.2	-	-
(717	15	0	b	1.02	78	9.2	-	-)

s = sharp, b = blunted

Table 3 Test conditions and results of base plate loading experiments, double crack configurations

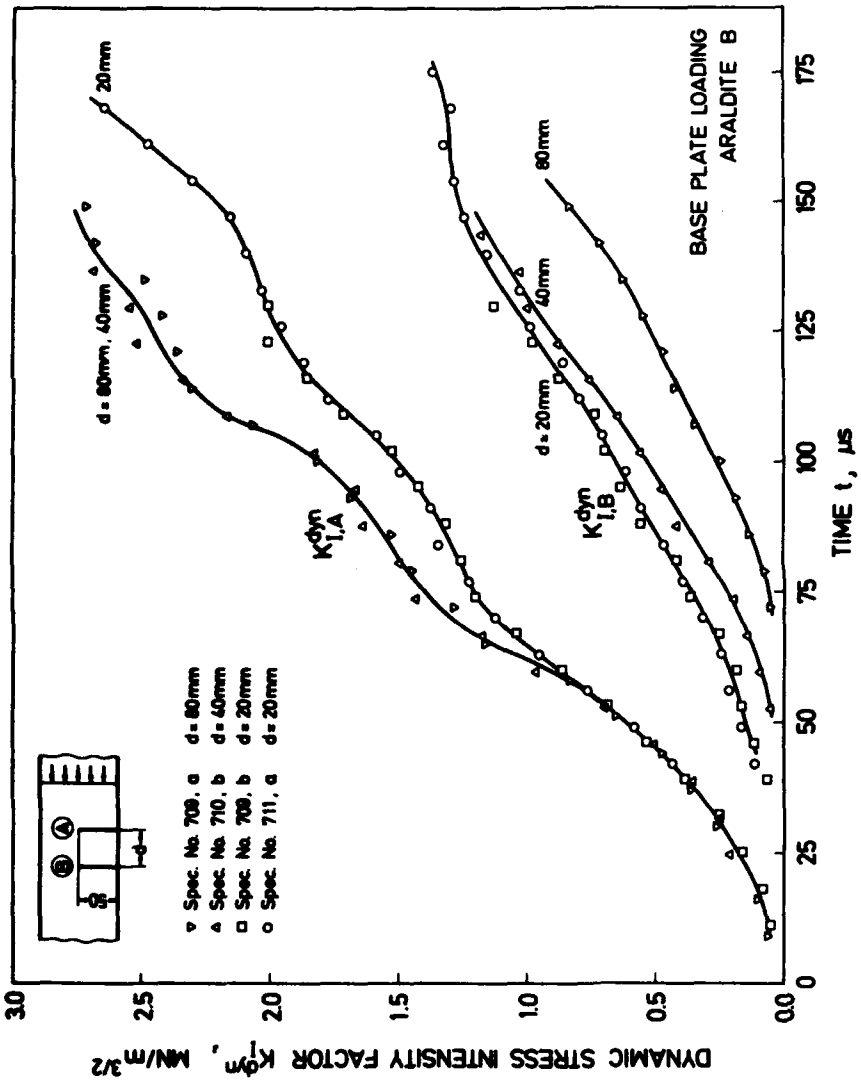

Fig. 28 Dynamic mode-I stress intensity factors for double crack configurations

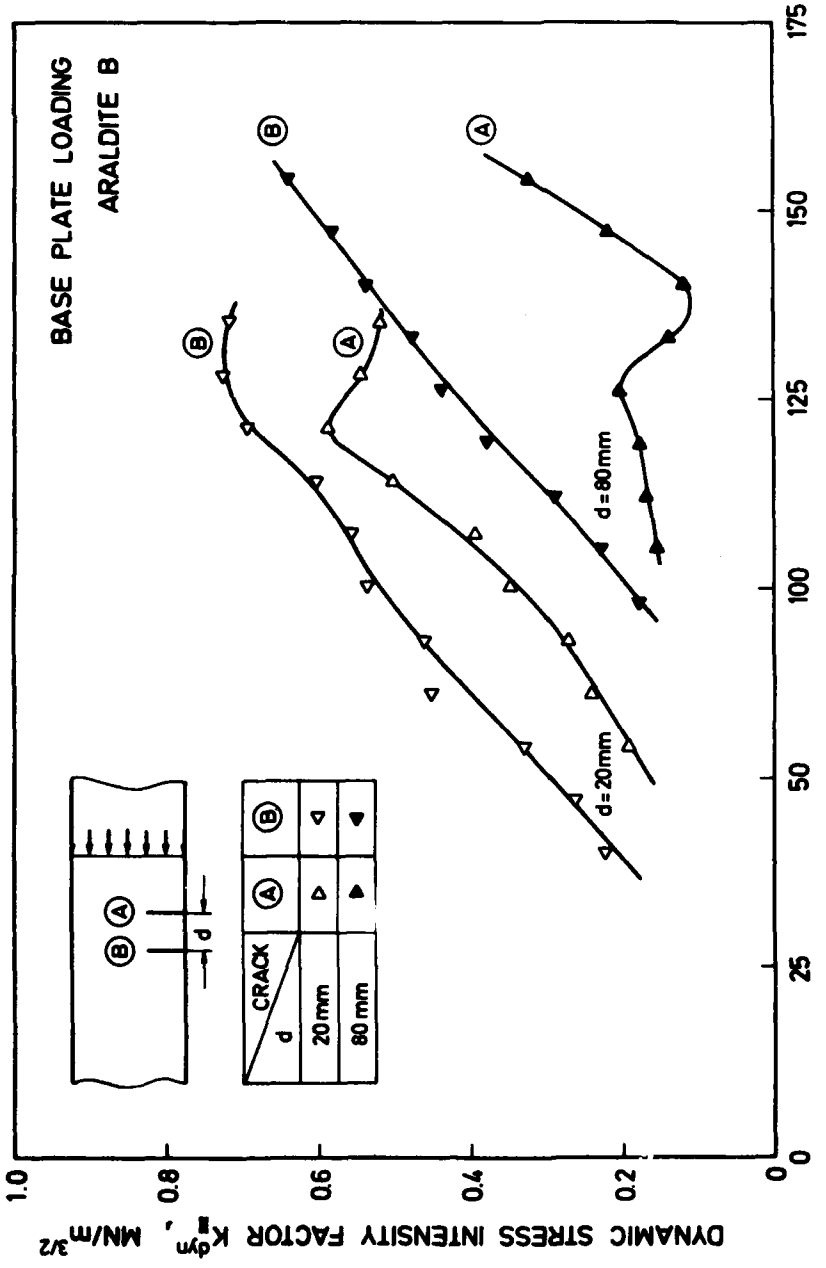

Fig. 29 Dynamic mode-II stress intensity factors for double crack configurations

clarity. The following trends can be recognized from the presented data: The stress intensity factors K_{II}^{dyn} of cracks B are larger than for cracks A. This result is plausible since crack B is loaded by a stress pulse which is disturbed by crack A from the very beginning on. Crack A, however, for a long time behaves as a single crack, which is not disturbed by crack B. The stress intensity factors K_I^{dyn} of the crack A are larger for the narrow (d = 20 mm) configuration than for the wider (d = 80 mm)crack configuration. Again this result is plausible since the interaction for the narrow crack configuration starts earlier and is stronger than for the wider crack configuration. This result is also in accordance with the observed reduction of crack A stress intensity factors for the narrow crack configuration at $t > 60$ µs (see discussion before). Thus, the data show a behavior which is in accordance with expectations. The observed scatter in the K_{II}-data was larger than for pure mode-I data. This larger scatter is partly due to the evaluation procedure for determining the data from the asymmetry of the caustics. The stress intensity factors are derived from the two longitudinal diameters D_{max} and D_{min} (see Fig. 9). Necessarily, however, the causticis are somewhat disturbed in the region where the caustic intersects the crack surfaces, i.e. where the asymmetry of the caustic is measured. The development of an improved evaluation procedure which takes unavoidable experimental disturbances of the caustic into account is planned.

Another series of experiments has been performed aimed to investigate the mutual interaction processes over a longer period of time. A further increase in crack tip bluntness did not lead to larger observation times. For crack tip radii $\gtrsim 1$ mm an initiation stress intensity factor of about 3 $MN/m^{3/2}$ was observed which could not be increased by a further increase in crack tip bluntness. Therefore, notches with reduced crack lengths have been utilized in order to reduce the stress intensity factor level.

A series of shadow optical photographs for a double crack configuration, d = 20 mm, a_o = 25 mm, is shown in Fig. 30. The tensile stress pulse impinges from the right side. For early times the crack A stress intensity factors are larger than the crack B stress intensity factors. This result is in accordance with the results discussed before. At later times, however, the situation changes. At 330 µs both caustics are of same size, i.e. the stress intensity factors are the same, and for larger times the situation is reversed and the crack B stress intensity factors are larger than the crack A stress intensity factors. Obviously an oscillation process takes place and the strain energy at the tip of one crack is transferred to the other.

Quantitative data for the crack configuration d = 20 mm, a_o = 15 mm are shown in Fig. 31. The stress intensity factors for crack A and crack B are shown as functions of time. In addition the behavior of an equivalent single crack is shown. At early times the crack A shows a similar behavior as the single crack, and crack B is only less loaded. Some time later (at ~100 µs), however, the situation has changed and

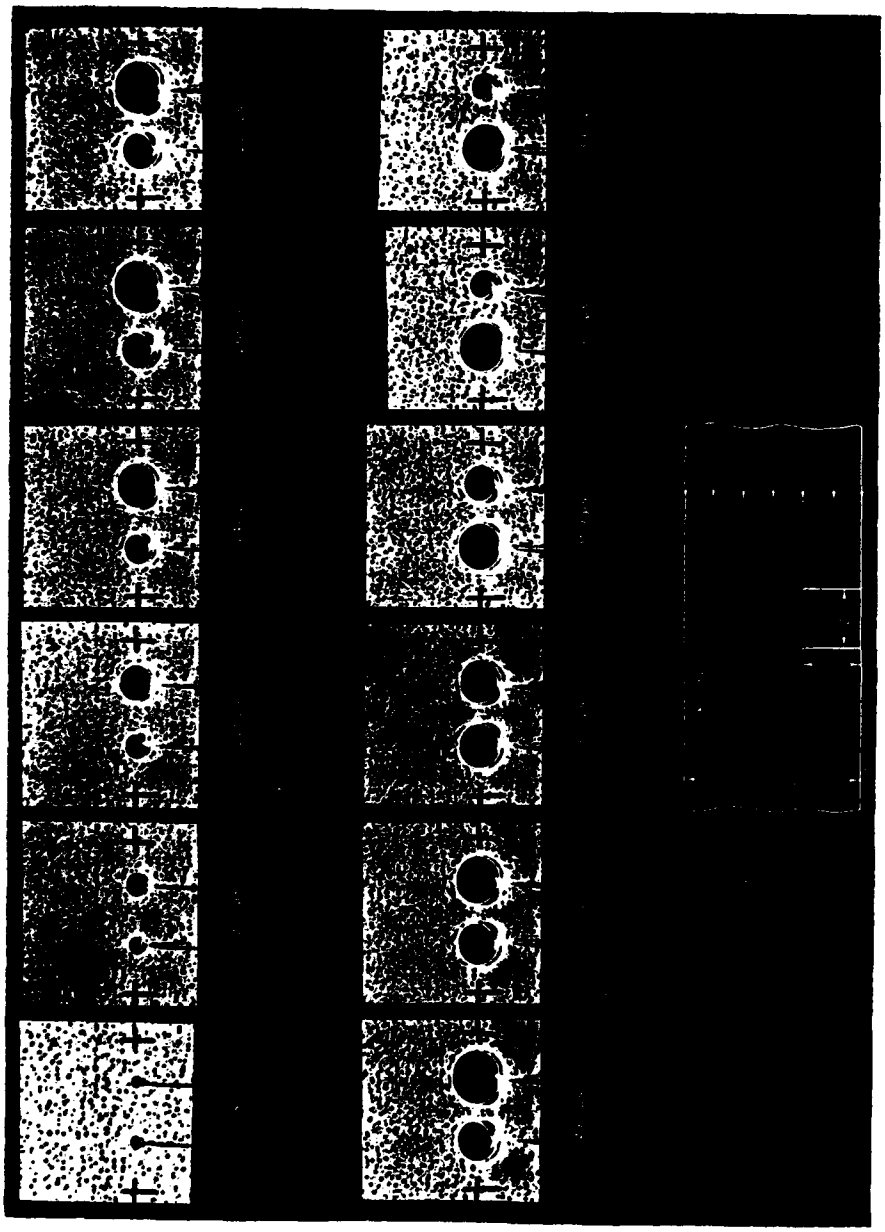

Fig. 30 Dynamic interaction of a double crack configuration

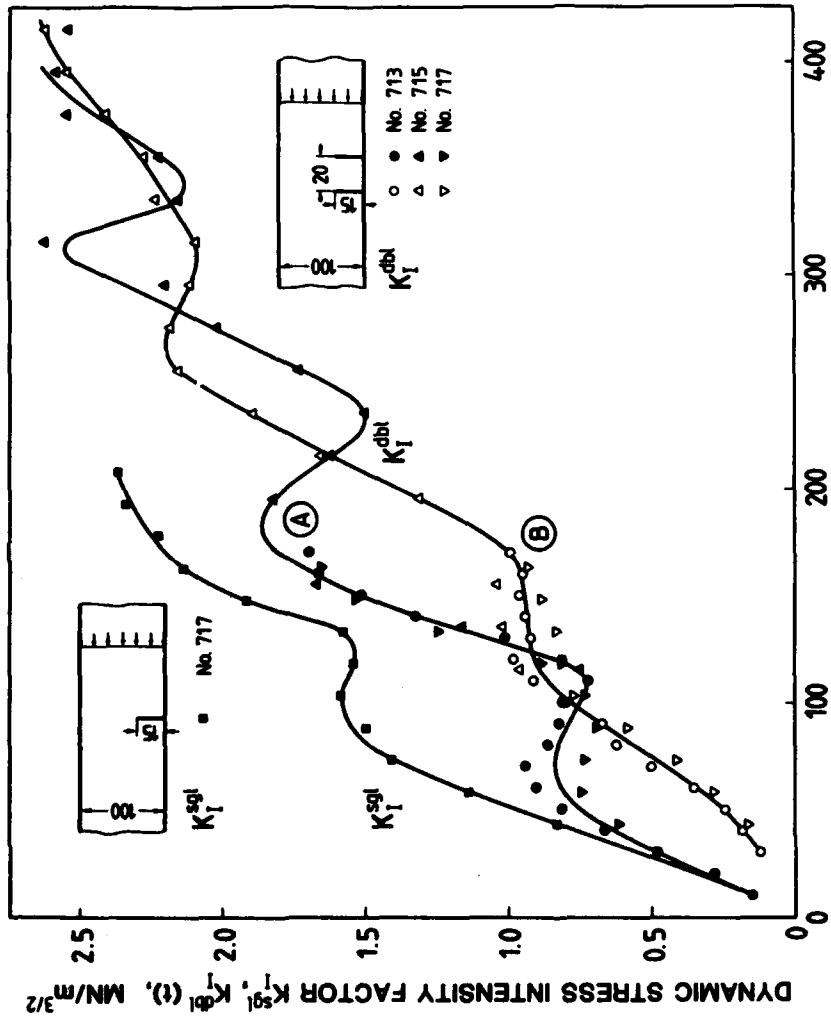

Fig. 31 Dynamic stress intensity factors for a double crack configuration in comparison to an equivalent single crack

crack B exhibits the larger stress intensity factor. Data at larger times show that this process varies periodically. At very large times the average stress intensity factor of the two parallel cracks is smaller than the one of the single crack, similar as in the static case.

These data show that predictions on dynamic fracture processes on the basis of simplified static analyses can only be considered as reasonable approximations for times which are considerably large. In the transient regime the situation is much more complex and static predictions can be very misleading.

5 INDEPENDENCE OF THE STRESS INTENSITY FACTOR FORM CRACK LENGTH

Stress intensity factor histories for cracks of different lengths which were impacted under similar conditions have been measured and compared with each other. In order to allow for an easy survey and to avoid a consideration of too many parameters only the results of single edge cracks shall be discussed here. Fig. 32 shows data for cracks 50 mm and 15 mm long, loaded in the base plate arrangement (see Chapter 3.1) at about 10 m/s. The stress intensity factors K_I^{dyn} are plotted as functions of time. It is recognized that the stress intensity factors for the two cracks of different length are identical till about 80 µs. Only for longer times the larger crack shows a larger stress intensity factor as one would expect from static considerations. In the early time regime, however, the stress intensity factors are obviously independent of crack length. This experimental result is in accordance with earlier theoretical predictions. Sih et al. [5,9], Achenbach [6,7] and Freund [8] calculated the stress intensity factor histories for cracks under step function loads (see Fig. 2) and showed that the stress intensity factors should increase according to a square root of time relationship, independent of crack lenghts for $t \lesssim a_0/c_1$ (see also Chapter 1). In their minimum time fracture criterion, Kalthoff and Shockey [14-17] state that cracks which are loaded by stress pulses of finite durations T_0 should show instability stresses which are independent of crack length if $T_0 < 2\ a_0/c_1$. Only for $T_0 > 30\ a_0/c_1$ static predictions would be applicable. The data reported in Fig. 32 indicate an independent stress intensity factor behavior for times $t < 80$ µs, i.e. $13\ a_0/c_1$. It is interesting to recognize that this value is in the range of the theoretical predictions although the loading conditions in the reported experiments were different from the ones considered in the theoretical analyses and thus do not allow for a direct comparison of data.

6 SUMMARY

Within the second year of the three year's research project many experiments of the proposed main investigations have been carried out.

First the dependence of the impact fracture toughness K_{Id} on loading rate has been investigated. Specimens made from Araldite B with single edge cracks have been tested under base plate and under direct impact

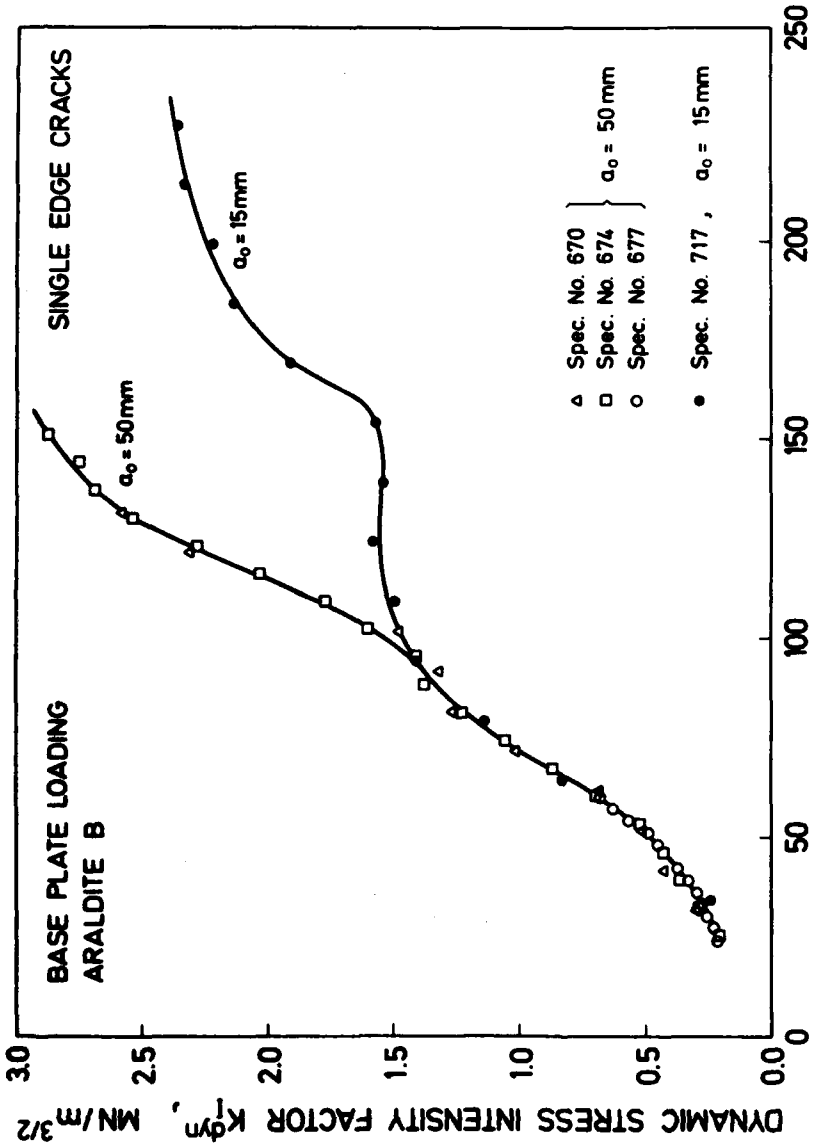

Fig. 32 Dynamic stress intensity factors for cracks of different lengths

loading conditions. Within the range of loading rates achieved so far, the measured impact fracture toughness data K_{Id} do not show a dependence from loading rate.

The experiments with configurations of multiple cracks exhibit a rather complex time dependent stress intensity factor history. Due to transient effects the early time behavior is very different from the static behavior. In particular a periodic exchange of the crack tip strain energy from one crack to the other takes place. Only for long times after impact the overall situation becomes similar to the one under static loading conditions.

The stress intensity factor histories for cracks of different lengths under impact loading has been measured and compared. The data do not show an influence of crack length for early times after impact. Only at later times the larger crack exhibits a larger stress intensity factor, as one expects from static considerations. Thus the parameter "time" controlles the fracture behavior under highly dynamic loading conditions and not the length of the crack as in static considerations.

In the next reporting period the K_{Id}-investigations with Araldite B specimens will be supplemented by further impact experiments performed under direct loading conditions. In these experiments the impact velocities will be increased to values up to 40 m/s in order to further reduce the resulting time to fracture. Predominantly, however, experimentswith high strength steel specimens will be performed utilizing the shadow optical method of caustics in reflection. Since this material is more strain rate sensitive and since the impact velocities can be increased to higher values more informative data on the K_{Id}-behavior at high loading rates are expected.

7 REFERENCES

[1] ASME Boiler and Pressure Vessel Code, The American Society of Mechanical Engineers, New York, N.Y., U.S.A.

[2] ASTM Book of Standards, Part 10, American Society for Testing and Materials, Philadelphia, Pa., U.S.A.

[3] ASTM E 24.03.03, "Proposed Standard Method of Tests for Instrumented Impact Testing of Precracked Charpy Specimens of Metallic Materials", Draft 2c, American Society for Testing and Materials, Philadelphia, U.S.A., 1980

[4] Kalthoff, J.F., Böhme, W., Winkler, S., and Klemm, W.: "Measurements of Dynamic Stress Intensity Factors in Impacted Bend Specimens", CSNI Specialist Meeting on Instrumented Precracked Charpy Testing, EPRI, Palo Alto, Calif., U.S.A., Dec. 1980

[5] Sih, G.C.: "Some Elastodynamic Problems of Cracks", Int. J. Fract. Mech. 4, 1968, 51-68

[6] Achenbach, J.D.: "Brittle and Ductile Extension of a Finite Crack by a Horizontally Polarized Shear Wave", Int. J. Engng. Sci. 8, 1970, 947-966

[7] Achenbach, J.D.: "Dynamic Effects in Brittle Fracture", Mechanics Today, Vol. 1, 1972, ed. by Nemat-Nasser, Pergamon

[8] Freund, L.B.: "Crack Propagation in an Elastic Solid Subjected to General Loading - III. Stress Wave Loading", J. Mech. Phys. Solids 21, 1973, 47-61

[9] Sih, G.C.: "Handbook of Stress Intensity Factors", Institute of Fracture and Solid Mechanics, 1973, Lehigh University, Bethlehem, Pa., U.S.A.

[10] Steverding, B., Lehnigk, S.H.: "Response of Cracks to Impact", J. Appl. Phys. 41, 1970, 2096-2099

[11] Steverding, B., Lehnigk, S.H.: "Collision of Stress Pulses with Obstacles and Dynamics of Fracture", J. Appl. Phys. 42, 1971, 3231-3238

[12] Lehnigk, S.H.: "A Macroscopic Dynamic Theory of Stability and Instability of Cracks Under Impulsive Loading", Dynamic Crack Propagation, ed. by G.C. Sih, Noordhoff-Groningen, 1973, 333

[13] Steverding, B.: "Fracture and Dislocation Dynamics", Dynamic Crack Propagation, ed. by G.C. Sih, Noordhoff-Groningen, 1973, 349

[14] Kalthoff, J.F., Shockey, D.A.: "On the Dynamic Instability of Cracks Loaded by Tensile Stress Pulses of Short Duration", Poulter Laboratory, Technical Report 001-75, 1974, Stanford Research Institute, Menlo Park, California

[15] Shockey, D.A., Kalthoff, J.F.: "Stability of Cracks Under High Rate Loads", Joint JSME-ASME Applied Mechanics Western Conf., 24-27 March 1975, Waikiki Beach, Honolulu, Hawai

[16] Kalthoff, J.F., Shockey, D.A.: "Instability of Cracks Under Impulse Loads", Journ. Appl. Phys. 48, 1977, 986-993

[17] Shockey, D.A., Kalthoff, J.F., and Ehrlich, D.C.: "Evaluation of Dynamic Crack Instability Criteria", Int. J. Fracture, Vol. 22, 1983, 217-229

[18] ASTM SPT 466 "Impact Testing of Metals", American Society for Testing and Materials, Philadelphia, Pa., 1974, U.S.A.

[19] ASTM STP 563 "Instrumented Impact Testing", American Society for Testing and Materials, Philadelphia, Pa., 1974, U.S.A.

[20] Shoemaker, A.K., Rolfe, S.T.: "The Static and Dynamic Low-Temperature Crack Toughness Performance of Seven Structural Steels", J. Engng. Fract. Mech., Vol. 2, 1971, 319-339

[21] Loss, J.F., Hawthorne, J.R., Griffis, C.A.: "Fracture Toughness of Light Water Reactor Pressure Vessel Materials", Naval Research Laboratory Memorandum Report 3036, 1975

[22] Proc. Int. Conf. Dynamic Fracture Toughness, London, July 5-7 1976

[23] Costin, L.S., Duffy, J., and Freund, L.B.: "Fracture Initiation in Metals Under Stress Wave Loading Conditions", ASTM STP 627, Fast Fract. and Crack Arrest, American Society for Testing and Materials. Philadelphia, Pa., U.S.A., 1977, 301

[24] Costin, L.S., Server, W.L., Duffy, J.: "Dynamic Fracture Initiation: A Comparison of Two Experimental Methods", to be published in ASME, J. of Engng. Materials and Technology

[25] Shockey, D.A., Curran, D.R.: "A Method for Measuring K_{Ic} at Very High Strain Rates", ASTM STP 536, American Society for Testing and Materials, Philadelphia, Pa., U.S.A., 1973, 297

[26] Homma, H., Shockey, D.A., and Muragama, Y.: "Response of Cracks in Structural Materials to Short Pulse Loads", submitted to J. Mech. Phys. Solids

[27] Shockey, D.A., Kalthoff, J.F., Homma, H., and Ehrlich, D.C., "Response of Cracks to Short Pulse Loading", Workshop on Dynamic Fracture, Ed. W.G. Knauss, California Institute of Technology, Pasadena, Calif., U.S.A., February 17-18, 1983

[28] Ravi Chandar, K., and Knauss, W.G.: "Dynamic Crack-Tip Stresses under Stress Wave Loading - A Comparison of Theory and Experiment" to appear in Int. Journ. of Fracture

[29] Eftis, J., Krafft, J.M.: "A Comparison of the Initiation with the Rapid Propagation of a Crack in a Mild Steel Plate", J. Basic Eng., 1965, 257

[30] Manogg, P.: "Anwendung der Schattenoptik zur Untersuchung des Zerreißvorgangs von Platten", Dissertation, Universität Freiburg, Germany, 1964

[31] Manogg, P.: "Schattenoptische Messung der spezifischen Bruchenergie während des Bruchvorgangs bei Plexiglas", Proceedings, International Conference on the Physics of Non-Crystalline Solids, Delft, The Netherlands, 1964, pp. 481-490

[32] Theocaris, P.S.: "Local Yielding Around a Crack Tip in Plexiglas", J. Appl. Mech., Vol. 37, 1970, pp. 409-415

[33] Beinert, J. and Kalthoff, J.F.: "Experimental Determination of Dynamic Stress Intensity Factors by Shadow Patterns" in Mechanics of Fracture, Vol. 7, Ed. G.C. Sih, Martinus Nijhoff Publishers, The Hague, Boston, London, 1981, pp. 281-330

[34] Kalthoff, J.F.: "Stress Intensity Factor Determination by Caustics", Intl. Conf. Experimental Mechanics, Society for Experimental Stress Analysis and Japan Society of Mechanical Engineers, Honolulu, Maui, Hawaii, U.S.A., May 23-28, 1982

[35] Kalthoff, J.F., Beinert, J., and Winkler, S.: "Measurements of Dynamic Stress Intensity Factors for Fast Running and Arresting Cracks in Double-Cantilever-Beam-Specimens", ASTM STP 627 - Fast Fracture and Crack Arrest, American Society for Testing and Materials, Philadelphia, U.S.A., 1977, pp. 161-176

[36] Kalthoff, J.F., Beinert, J., Winkler, S., and Klemm, W.: "Experimental Analysis of Dynamic Effects in Different Crack Arrest Test Specimens", ASTM STP 711 - Crack Arrest Methodology and Applications, American Society for Testing and Materials, Philadelphia, U.S.A., 1980, pp. 109-127

[37] Kalthoff, J.F., Beinert, J., Winkler, S.: "Analysis of Fast Running and Arresting Cracks by the Shadow Optical Method of Caustics", Symposium on Optical Methods of Mechanics of Solids, International Union of Theoretical and Applied Mechanics (IUTAM) Poitiers, France, Sept. 1979

[38] Kalthoff, J.F., Böhme, W., and Winkler, S.: "Analysis of Impact Fracture Phenomena by Means of the Shadow Optical Method of Caustics", VIIth Intl. Conf. Experimental Stress Analysis, Society for Experimental Stress Analysis, Haifa, Israel, Aug. 23-27, 1982

[39] Kalthoff, J.F., Winkler, S., Böhme, W. and Klemm, W.: "Determination of the Dynamic Fracture Toughness K_{Id} in Impact Tests by Means of Response Curves", 5th Intl. Conf. Fracture, Cannes, March 29 - April 3, 1981, Advances in Fracture Research, Ed. D. Francois et al., Pergamon Press, Oxford, New York, 1980

[40] Theocaris, P.S.: "Complex Stress-Intensity Factors at Bifurcated Cracks", J. Mech. Phys. Solids 20, 1972, 265-279

[41] Seidelmann, U.: "Anwendung des schattenoptischen Kaustikenverfahrens zur Bestimmung bruchmechanischer Kennwerte bei überlagerter Normal- und Scherbeanspruchung", IWM-Report 2/76, Fraunhofer-Institut für Werkstoffmechanik, Freiburg, 1976

[42] Beinert, J., Kalthoff, J.F., Seidelmann, U., and Soltész, U.: "Das schattenoptische Kaustikenverfahren und seine Anwendung in der Bruchmechanik", VDI-Berichte Nr. 207, pp. 15-25, VDI-Verlag, Düsseldorf, 1977

[43] Kalthoff, J.F., and Winkler, S., "Fracture Behavior under Impact", First Annual Report, W 8/83, prepared for European Research Office of the U.S. Army, London under Contract DAJA 37-81-C-0013, Fraunhofer-Institut für Werkstoffmechanik, Freiburg, West-Germany

[44] Ravi Chandar, K., and Knauss, W.G.: private communication

[45] Kalthoff, J.F.: "On Some Current Problems in Experimental Fracture Dynamics", Workshop on Dynamic Fracture, sponsored by NSF and ARO, W.G. Knauss, Ed., Calif. Inst. of Technology, Pasadena, Calif., Feb. 17-18, 1983

END

FILMED

1-84

DTIC